Reducing the Bacterial Lag Phase Through Methylated Compounds: Insights from Algal-Bacterial Interactions

Martin Sperfeld[1]†, Delia A. Narváez-Barragán[1]†, Sergey Malitsky[2], Veronica Frydman[3], Lilach Yuda[1], Jorge Rocha[4], and Einat Segev[1]*

Affiliations:

[1]Department of Plant and Environmental Sciences, Weizmann Institute of Science; Rehovot, 7610001, Israel.

[2]Department of Life Sciences Core Facilities, Weizmann Institute of Science; Rehovot, 7610001, Israel.

[3]Department of Chemical Research Support, Weizmann Institute of Science; Rehovot, 7610001, Israel.

[4]Agricultura en Zonas Áridas, Centro de Investigaciones Biológicas del Noroeste, La Paz, Baja California Sur, Mexico.

*Corresponding author. Email: Einat.Segev@weizmann.ac.il

†These authors contributed equally to this work

Abstract: The bacterial lag phase is a key period for resuming growth. Despite its significance, the lag phase remains underexplored, particularly in environmental bacteria. Here, we explore the lag phase of the model marine bacterium *Phaeobacter inhibens* when it transitions from starvation to growth with a microalgal partner. Utilizing transcriptomics and ^{13}C-labeled metabolomics, our study reveals that methylated compounds, which are abundantly produced by microalgae, shorten the bacterial lag phase. Our findings underscore the significance of methyl groups as a limiting factor during the lag phase and demonstrate that methyl groups can be harvested from algal compounds and assimilated through the methionine cycle. Furthermore, we show that methylated compounds, characteristic of photosynthetic organisms, induce variable reductions in lag times among bacteria associated with algae and plants. These findings highlight the adjustability of the bacterial lag phase and emphasize the importance of studying bacteria in an environmental context.

One-Sentence Summary: Bacteria use algal compounds as a metabolic shortcut to transition from starvation to growth.

Introduction

Marine heterotrophic bacteria rely on organic carbon synthesized by photosynthetic microorganisms, and consume approximately half of the carbon fixed by these primary producers[1–3]. The primary producers, namely microalgae, produce organic carbon by fixing CO_2 in a process that is subjected to temporal dynamics[4,5]. For example, photosynthetic productivity is poor at night and in winter, when light intensities decline, or nutrients are depleted. Consequently, heterotrophic bacteria must endure prolonged phases of starvation[6–8]. However, with the onset of microalgal productivity, bacteria must rapidly activate their metabolism. A rapid metabolic response is key for bacteria to outgrow co-occurring competitors[9–11].

The transition from starvation[12,13] and preparation for cell division occur during the lag phase[14]. Recent studies highlight that bacteria undergo a global metabolic reorganization during the lag phase[15] and synthesize essential building blocks (such as nucleotides and amino acids), which are then incorporated into larger macromolecules including DNA, RNA and proteins[16–18]. Some building blocks can be acquired from external sources and alleviate metabolic needs during the bacterial lag phase[18]. While the crucial preparatory lag period has been well-studied in human pathogens and in food-spoiling bacteria[15], much is unknown about the bacterial lag phase and its controls in the marine environment.

Several groups of marine heterotrophic bacteria, such as the common Roseobacter group[19], are often found in association with microalgae[1]. Much knowledge exists regarding the metabolic pathways through which bacteria utilize algal metabolites for growth[20,21]. However, there remains a significant knowledge gap regarding the early physiological response of bacteria upon encountering algae after a period of starvation. As bacteria often endure periods of starvation in nature[22], strategies to optimize the initial interaction with algal hosts could prove beneficial for the ecological success of marine bacteria. In this study, we sought to understand the post-starvation response of a model Roseobacter species, *Phaeobacter inhibens*, to microalgal metabolites and to determine the underlying mechanisms.

We analyzed the metabolism of *P. inhibens* while it grows with microalgae or is supplemented with selected microalgal metabolites. We discovered that methyl groups represent a metabolic "bottleneck" to bacterial growth even when ample carbon and nutrients are made available. Nano- to micromolar concentrations of methylated compounds, which are abundantly produced by microalgae[23–25], significantly shorten the lag phase of bacteria. This observation marks methylated compounds as a class of metabolites that reduces lag times. Specifically, compounds that can donate one-carbon groups to the bacterial metabolism induce reduction of the lag phase with no influence on the bacterial growth rate. To elucidate the mechanisms that underly lag phase shortening by methylated compounds, we explored the bacterial transcriptome during the lag phase, estimated cellular requirements for methyl groups, and analyzed the incorporation of ^{13}C-labeled methyl groups. Our results suggest that methyl group synthesis is a constraint during the bacterial lag phase, a limitation that can be alleviated by abundant algal metabolites. Our findings reveal the overlooked tunability of the bacterial lag phase and underscore the importance of studying bacterial physiology within an ecological context.

Results

Bacterial methyl group metabolism genes are highly expressed across growth phases during co-cultivation with algae

We first set out to investigate the metabolic response that is activated in *Phaeobacter inhibens* bacteria during co-cultivation with *Emiliania huxleyi* microalgae (also known as *Gephyrocapsa huxleyi*[26]). This algal-bacterial pair naturally co-occurs in the environment and was previously studied by us[27,28] and by others[29–31]. We analyzed the transcriptome of bacteria in co-cultures with algae—a condition under which bacteria rely entirely on algal-secreted metabolites for growth[27]. As a reference condition, we analyzed bacterial pure cultures that received glucose as a sole carbon source (figs. S1-S3, tables S1-S2, and data S1). Notably, comparing pure bacterial cultures under nutrient replete conditions with glucose as a sole carbon source, and bacteria in co-cultures that receive a continuous, complex, yet limited supply of algal metabolites, contains inherent limitations. Yet, such a comparison can highlight potentially important differences and serve as a hypothesis generator for further exploration.

Based on KEGG metabolic pathways definitions[32] we identified catabolic and anabolic processes that are highly expressed in bacteria during co-cultivation with algae. We found that genes involved in utilizing methylated compounds were among the 20 highest transcribed bacterial metabolic genes (Fig. 1A and data S1). Examples include a gene encoding a cobalamin-dependent methyltransferase (gene 3 in Fig. 1A), a gene encoding a formate—THF ligase (gene 29), and genes involved in spermidine synthesis (genes 1, 2 and 21). Methyl group metabolism emerged as a central process during bacterial growth with algae. Consequently, to identify relevant genes that might have escaped annotation in the KEGG database, we conducted a manual search for bacterial genes involved in metabolizing methylated compounds, culminating in a comprehensive list of 83 genes (table S3 and fig. S4). Differential gene expression (DE) analysis indicated that the identified genes were markedly upregulated in the presence of algae, compared to bacterial pure cultures grown with glucose (Fig. 1B, and data S1 for DE results of all genes). To portray the possible routes by which bacteria utilize methyl groups during interactions with algae, we overlaid the reactions encoded by the methyl group metabolism genes with our DE results (Fig. 1C). This schematic overview of methyl group metabolism, also termed one-carbon metabolism, highlights that bacteria harvest, dissimilate, and assimilate methyl groups during interactions with algae, suggesting that methylated compounds are a relevant resource for algal-associated bacteria.

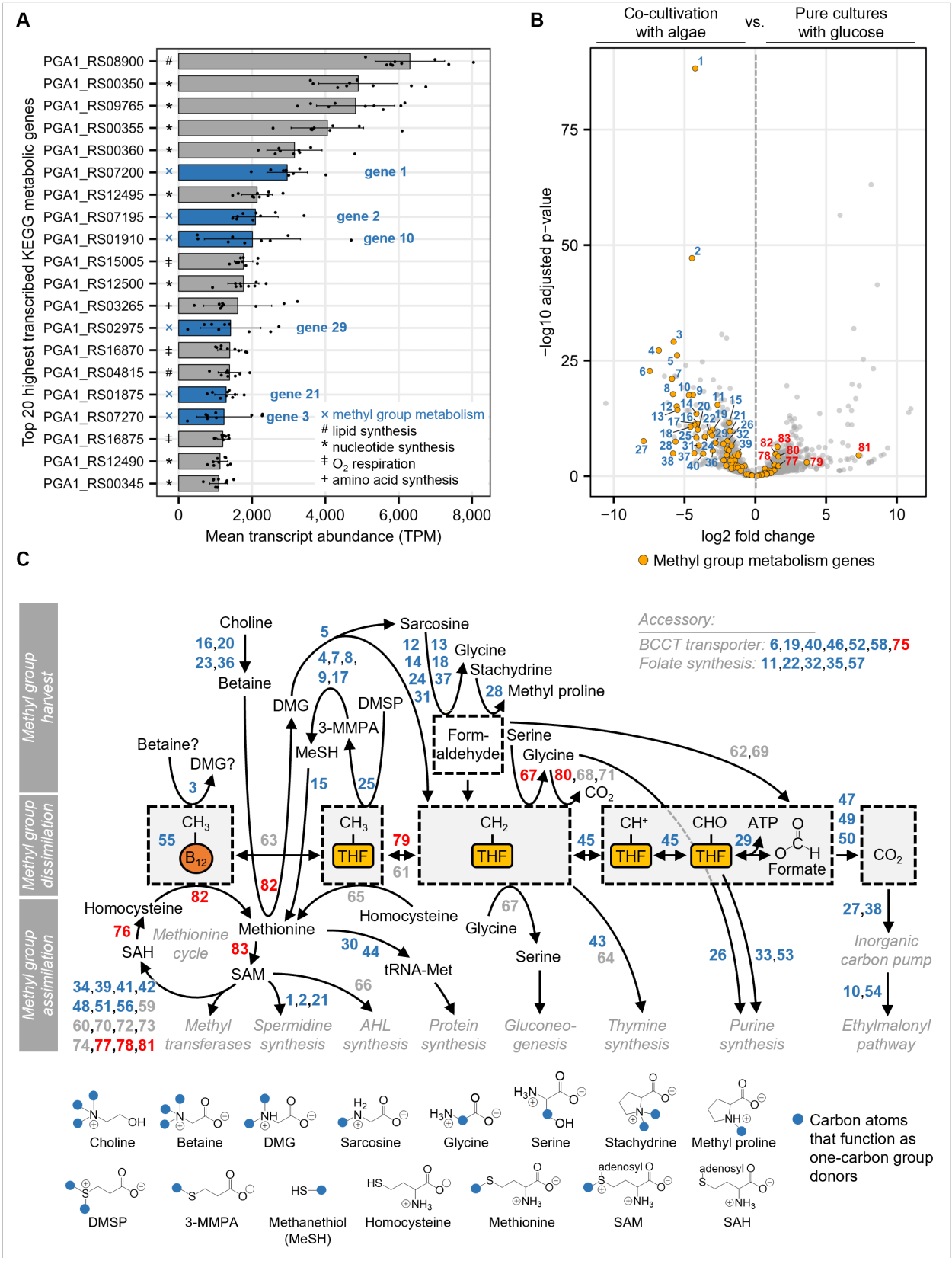

Fig. 1: Identification of metabolic genes that are transcribed in *P. inhibens* bacteria during co-cultivation with *E. huxleyi* microalgae. (**A**) Co-culture RNA-sequencing revealed that

bacterial genes involved in methyl group metabolism were among the highest transcribed KEGG metabolic genes in the presence of algae (blue bars). Bars represent the mean of nine algal-bacterial co-cultivation samples taken from three different time points (see fig. S1 for sampling points). Error bars depict standard deviations. Labels on the y-axis: RefSeq accession numbers. KEGG annotations of respective methyl group metabolism genes: *S*-adenosylmethionine decarboxylase (gene 1), trimethylamine—corrinoid protein Co-methyltransferase (gene 3), spermidine synthase (gene 2), crotonyl-CoA carboxylase/reductase (gene 10), formate—tetrahydrofolate ligase (gene 29), ornithine decarboxylase (gene 21). See data S1 for transcript abundances per sample. (**B**) Methyl group metabolism genes (orange dots) were upregulated in bacteria that were co-cultivated with algae (left; blue numbers) compared to bacteria in pure cultures that grew exponentially with glucose (right; red numbers). Samples used for differential gene expression analysis are presented in fig. S1. (**C**) Bacterial methyl group metabolism genes include reactions involved in harvesting, dissimilating and assimilating methyl groups from methylated donor compounds. Included are genes that are either directly involved in transforming methyl groups, or which are accessory and encode for transporters or tetrahydrofolate (THF) synthesis. Blue and red numbers indicate up- and downregulated genes, respectively (thresholds for coloring: adjusted p-value < 0.05; log2 fold change < -0.585 and > +0.585). Gene numbers are identical throughout the text and figures, with accession numbers and functional annotations listed in table S3. Blue dots in chemical structures represent carbon atoms (mainly methyl groups) that function as one-carbon group donors. BCCT—Betaine/Carnitine/Choline Transporter family.

The methylated compound DMSP triggers the shortening of the bacterial lag phase

To investigate the influence of methylated compounds on bacteria, we conducted a series of growth experiments using the methylated compound dimethylsulfoniopropionate (DMSP) as a model substrate. DMSP is naturally produced by microalgae and was extensively studied in the context of bacterial metabolism and growth[33,34]. In our experiments, bacterial pure cultures were pre-cultivated with glucose as a sole carbon source until reaching stationary phase. Then, stationary phase bacteria were used to initiate fresh cultures which contained the same glucose medium, but that were additionally supplemented with DMSP (or with water as control). We found that micromolar concentrations of DMSP stimulated the growth of bacteria (Fig. 2A). Plotting the growth curves semilogarithmically revealed that the low levels of added DMSP affected specifically the bacterial lag period; lag times were shortened while growth rates were not affected (Fig. 2B and fig. S5A). We further quantified the lag phase shortening effect by calculating △lag times, which is the time difference between the onset of growth in control cultures, compared to supplemented cultures (Fig. 2B and fig. S5B). By analyzing △lag times under different DMSP concentrations, we found that lag times were shortened by up to 2.5 hours, and that already nanomolar concentrations of DMSP resulted in significantly lower lag times (Fig. 2C and fig. S5C). Interestingly, above 20 μM a higher concentration did not increase the delta lag phase. This suggests that there may be a threshold at which the demethylation machinery becomes saturated, leading to diminished sensitivity to DMSP, as previously suggested[35].Our results show that in the presence of a utilizable carbon source such as glucose (provided at a concentration of 1 mM in our experiments), exposure to low levels of the methylated compound DMSP leads to the shortening of the bacterial lag phase.

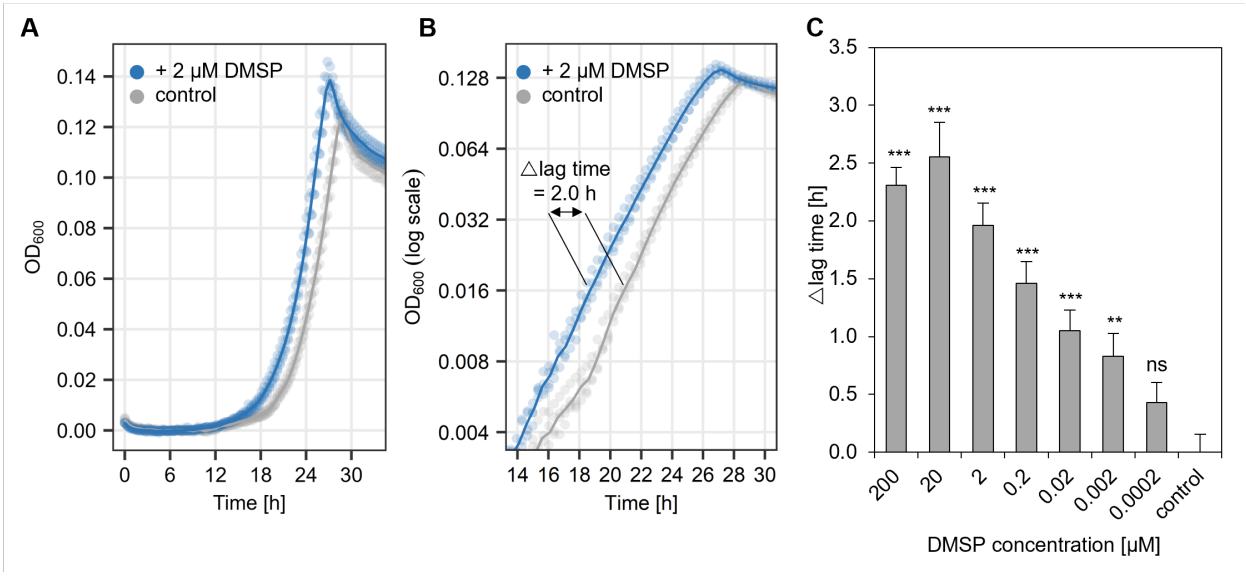

Fig. 2: The methylated compound DMSP induces lag phase shortening in *P. inhibens* bacteria. (**A**) Micromolar concentrations of DMSP stimulated earlier growth of bacteria (blue) compared to control cultures supplemented with water (grey). (**B**) Semi-log2 transformed growth curves show that doubling times were unchanged, as evident from the identical slopes, while lag times were shortened. Lag phase shortening is expressed as the difference between mean lag times measured for supplemented cultures compared to control cultures (△lag time; see *Method details* for explanations). (**C**) Exposure to nanomolar concentrations of DMSP resulted in significant bacterial lag phase shortening. All growth experiments were conducted in artificial seawater medium (ASW_b) with 1 mM glucose as carbon source, using glucose-grown, stationary phase pre-culture bacteria as inoculum. For each condition, four biological replicates were used (four wells of a 96-well plate were inoculated with the same pre-culture). In panels **A** and **B**, dots represent individual measurements for each of the four replicates per time point, and lines depict a smoothed average. Error bars in panel **C** indicate the standard deviation of the estimated difference between means. ANOVA and Dunnett's test were used to identify significant differences between control and supplemented cultures (adjusted *p*-value thresholds: *** ≤ 0.001, ** ≤ 0.01, ns [not significant] > 0.05).

Methyl groups are involved in lag phase shortening

To determine whether the methyl groups of DMSP are involved in lag phase shortening, we used analogues of DMSP that harbor different numbers of methyl groups (Fig. 3A and figs. S6-S7). We found that the extent of lag phase shortening correlated with the number of methyl groups per molecule, while non-methylated analogues did not have a measurable impact on the lag period (Fig. 3A and table S4 for statistical significance). This finding suggests that the methyl groups of DMSP drive lag phase shortening.

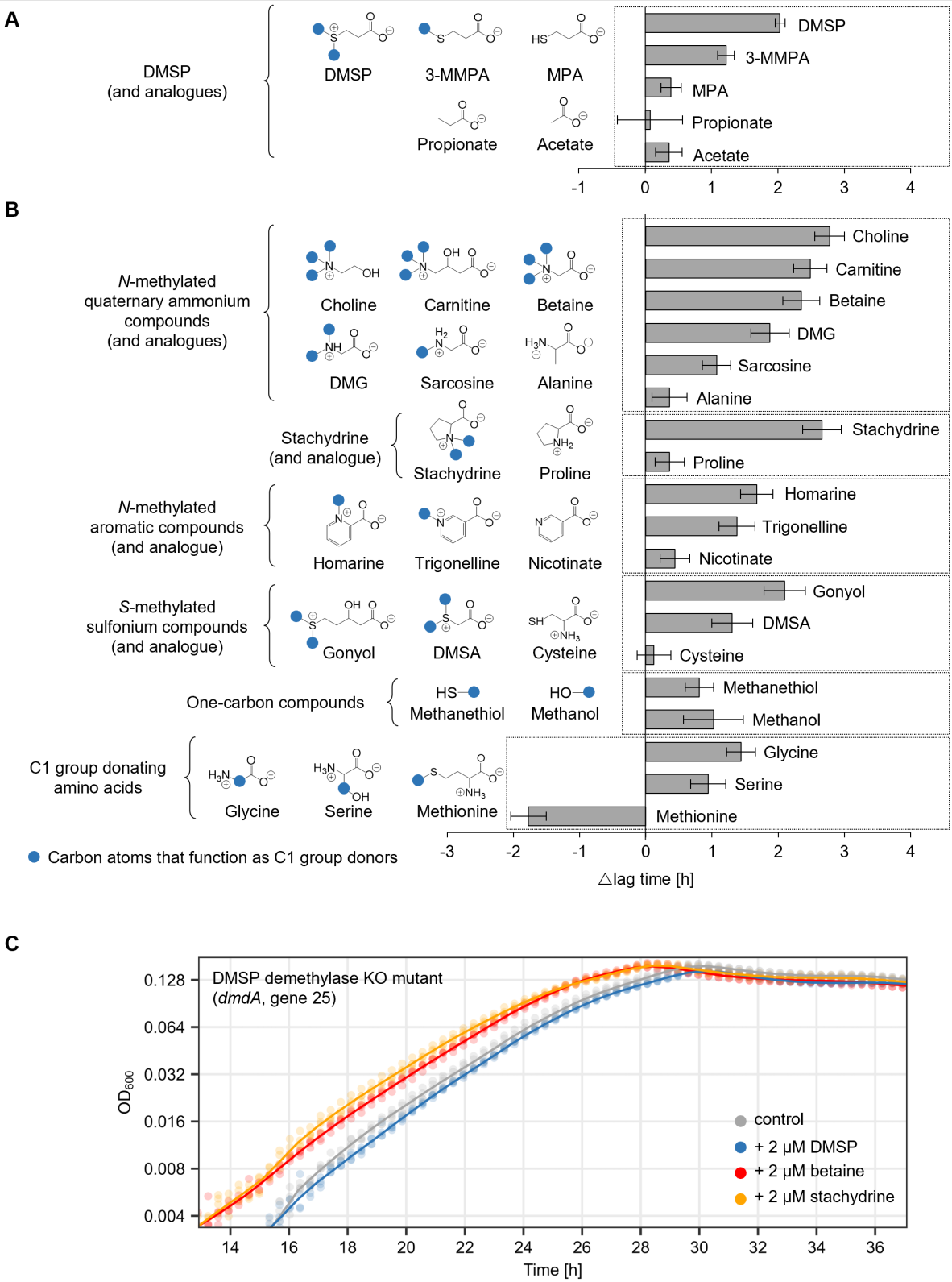

Fig. 3: Methyl groups and other one-carbon moieties induce lag phase shortening in *P. inhibens* bacteria. (**A**) Growth experiments with analogues of DMSP (2 µM) revealed that methyl groups are required for lag phase shortening. The number of methyl groups per molecule

correlated with the extent of lag phase shortening. (**B**) Growth experiments further revealed that multiple methylated compounds (2 μM) trigger lag phase shortening, while non-methylated analogues at the same concentration were less or not effective. In panels (**A**) and (**B**), blue dots in chemical structures represent carbon atoms (mainly methyl groups) that function as one-carbon group donors. Bars represent differences between mean lag times measured for supplemented cultures compared to control cultures (△lag time). Each condition was analyzed with three biological replicates, and error bars indicate standard deviation of the difference between estimated means. (**C**) Lag phase shortening was no longer evident in a *P. inhibens dmdA* knock-out mutant upon exposure to DMSP, while other methylated compounds (betaine and stachydrine) still triggered lag phase shortening. Dots represent individual measurements for four biological replicates, and lines depict a smoothed average.

To substantiate the role of methyl groups, we investigated whether other methylated compounds that are commonly produced by microalgae induce lag phase shortening (Fig. 3B). We selected methylated compounds with different chemical properties including *N*-methylated, *S*-methylated, small one-carbon compounds and amino acids (which are themselves not methylated but that can donate one-carbon groups to the cellular methyl group metabolism). All compounds were added at a concentration of 2 μM. The results show that supplementation with all tested methylated compounds resulted in shortening of the lag phase (Fig. 3B and table S4 for statistical significance), while the doubling times were largely unchanged (figs. S6-S7). The extent of lag phase shortening correlated with the number of methyl groups per molecule, in line with our results with the DMSP analogues (Fig. 3A). Interestingly, methionine was an exception and prolonged the lag phase. Growth inhibitions by methionine were reported for other bacteria and may result from feedback loops that regulate intracellular methionine concentrations[36]. In summary, our findings demonstrate that different methylated compounds prompt a reduction in the bacterial lag phase and suggest a correlation between the quantity of methyl groups present in a compound and the degree of lag reduction. Furthermore, the data also reveal that additional characteristics of the tested compounds, such as carbon count or the nature of chemical moieties (*N*-methylated versus *S*-methylated), do not influence the shortening of the lag phase. This underscores the centrality of methyl groups in the process of lag phase shortening.

Harvesting the methyl group from a methylated compound is required for lag phase shortening

The involvement of methyl groups in lag phase shortening could be explained by three possible scenarios: 1) methyl groups are a limiting resource, 2) methylated compounds are sensed by receptor proteins that trigger a signal cascade, and 3) methylated compounds act as intracellular solutes with protective functions. To distinguish between these possibilities, we generated a *P. inhibens* knock-out (KO) mutant that is unable to harvest methyl groups from a respective donor compound. We deleted the *dmdA* gene (Fig. 1C; gene 25), which encodes for the well-characterized DMSP demethylase[37]. The deletion of the demethylase gene is expected to hamper the harvest of methyl groups from DMSP, while it is not expected to affect extracellular receptor binding or internalization of the compound. Our data show that DMSP-dependent lag phase shortening was abolished in the *dmdA* KO mutant (Fig. 3C). Importantly, the mutant still demonstrated lag phase shortening when supplemented with other methylated compounds (Fig. 3C). Interestingly, we observed a more pronounced difference in the reduction of the lag phase due to altered amounts of methyl groups on DMSP (Fig. 3A) compared to changes in the concentration of the added DMSP (Fig. 2C). While the molecular mechanisms underlying this

difference are not fully understood, a possible explanation previously suggested is the insensitivity of DMSP catabolic enzymes to increasing levels of DMSP[35]. Additionally, DMSP and other methylated compounds are compatible solutes and are transported into the cell via high-affinity transport systems[38]. These transporters function effectively at low substrate concentrations but become saturated at higher concentrations, potentially contributing to diminished lag reductions with increasing DMSP concentrations. While the DMSP demethylase is a well-studied enzyme, its role in lag phase dynamics has been overlooked. These results suggest that methyl groups are a limiting resource during the lag phase and that bacteria can overcome this bottleneck by harvesting methyl groups from external donor compounds.

Stoichiometric calculations highlight assimilatory methyl group requirements

Methyl groups may function as a limiting resource either by being assimilated as a one-carbon group (C1) substrate, or by being dissimilated for ATP generation (Fig. 1C). To explore the possible fate of methyl groups during the lag phase, we estimated the C1 group requirements per bacterial cell needed for one cell duplication. In this process, C1 groups are utilized as a substrate to synthesize cellular building blocks for biomass formation (i.e., purines, thymine, methionine and histidine; table S5). Based on numbers determined for exponentially growing *E. coli*[39], we calculated that a single *P. inhibens* cell requires 190.1 amol of C1 groups to synthesize the building blocks needed for one cell duplication (table S5). If a freshly initiated *P. inhibens* culture, at a density of 25,000 CFU/mL, assimilates all available DMSP methyl groups during the lag phase, then the bacterial population requires 2.4 nM of DMSP to duplicate. Indeed, similar DMSP concentrations—2 nM—induced significant lag phase shortening (Fig. 2C).

Methyl groups can also undergo dissimilation to generate ATP, producing one ATP per methyl group (Fig. 1C; gene 29). According to the provided growth-associated maintenance cost (GAM) in the metabolic model of *P. inhibens*[40], a single *P. inhibens* cell requires 23,800 amol ATP to conduct one cell duplication during exponential growth with glucose. If a freshly initiated *P. inhibens* culture (25,000 CFU/mL) were to rely entirely on the dissimilation of DMSP methyl groups during the lag phase to meet its ATP requirements, the bacterial population would need 298 nM of DMSP to fulfill 100% of the ATP costs for one duplication. In our experiments, 2 nM DMSP already induced significant lag phase shortening (Fig. 2C). This concentration can cover only 0.7% of the bacterial ATP needs. It is important to acknowledge that the presented values in this calculation are estimations and may likely underestimate bacterial requirements. However, it is noteworthy that the difference in assimilatory versus dissimilatory needs, which can be both fulfilled by methyl groups, spans two orders of magnitude. Despite potential biases in our estimations, this calculation highlights the considerable potential of methyl groups to alleviate assimilatory needs and accelerate the lag phase, rather than substantially affecting the high demand of dissimilatory processes. Based on these calculations, it appears more plausible that methyl groups are assimilated during the lag phase to cover C1 group requirements, while the required ATP is generated from the glucose in the medium.

Methyl group assimilation genes are upregulated during the lag phase

To experimentally elucidate the intracellular fate of methyl groups, we analyzed the bacterial transcriptome in response to DMSP specifically during the lag phase. If methyl groups are indeed assimilated during the lag phase, functions associated with methyl group assimilation are

anticipated to be transcriptionally regulated during this phase. The transcriptome of *P. inhibens* was previously demonstrated to be remarkably dynamic, revealing rapid responses occurring within minutes following treatment[41]. Therefore, RNA was sampled 15 min and 40 min after initiation of fresh cultures, using glucose-grown stationary phase bacteria as inoculum. The cultures contained either glucose as sole carbon source or were supplemented with DMSP (figs. S8-S10, tables S6-S7 and data S2). Our data show that the addition of DMSP resulted in the upregulation of 43 methyl group metabolism genes during the lag phase and the downregulation of 12 genes (figs. S11-S13)—an effect that was most pronounced 15 min post initiation of fresh cultures.

Specifically, genes involved in DMSP catabolism were upregulated (fig. S11; genes 4, 7, 8, 9, 17, 25), including the DMSP demethylase gene (*dmdA*: gene 25). The most upregulated genes were involved in synthesizing spermidine (fig. S11; genes 1, 2 and 21), which is a metabolite associated with cell growth[42]. The most downregulated gene was involved in methyl group oxidation—a regulation that may impede methyl group dissimilation (fig. S11; gene 79). Interestingly, DMSP demethylation (*dmdA*: gene 25), spermidine synthesis (*speD*: gene 1, *speE*: gene 2, and gene 21) and methyl group oxidation (*metF*: gene 79) are all linked via the methionine cycle (Fig. 4A). This link is further supported by the upregulation of *metK* (gene 83)—a gene that is involved in converting methionine into *S*-adenosylmethionine (SAM; Fig. 4A). In summary, transcriptome analyses suggest that DMSP methyl groups are assimilated during the bacterial lag phase through the methionine cycle.

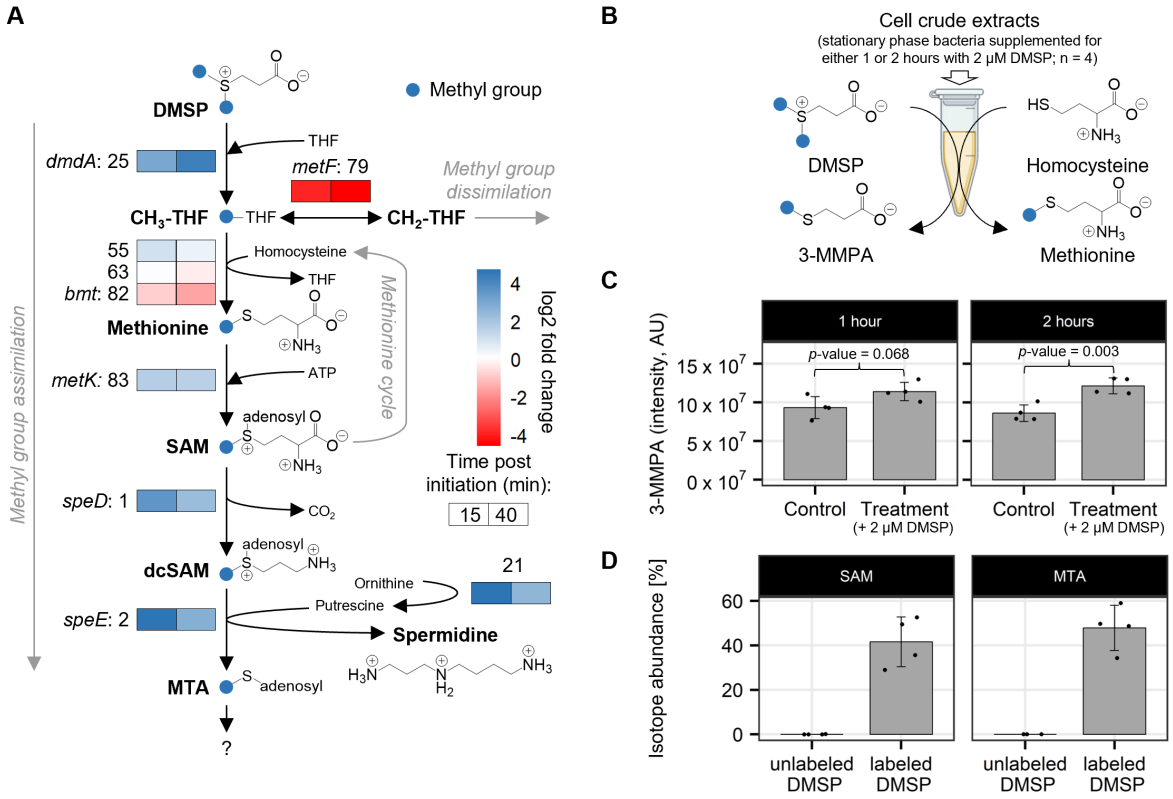

Fig. 4: Transcriptional, metabolic and enzymatic response of *P. inhibens* bacteria towards DMSP during the lag phase. (**A**) The transcriptional response was analyzed in freshly initiated bacterial cultures that were supplemented with 50 µM DMSP, compared to control cultures

without DMSP (all cultures contained 1 mM glucose; fig. S8). Gene expression changes (log2 fold change) are indicated as colored boxes that correspond to the age of the culture post initiation—15 min (left box) and 40 min (right box). Colors show upregulation (blue) and downregulation (red) in response to DMSP. The three most upregulated methyl group metabolism genes were involved in spermidine synthesis (*speD*: gene 1, *speE*: gene 2, and gene 21; fig. S11). Spermidine synthesis utilizes *S*-adenosylmethionine (SAM), which is the main product of the methionine cycle. Likewise, genes involved in DMSP demethylation (*dmdA*: gene 25; fig. S11) and SAM synthesis (*metK*: gene 83; fig. S11) were highly upregulated in response to DMSP. A gene that mediates between methyl group assimilation and dissimilation was the most downregulated gene in response to DMSP (*metF*: gene 79; fig. S11). Numbers left to boxes or above designate gene numbers (see table S3 for accession numbers and functional annotations). RNA-sequencing was conducted using three biological replicates per condition. (**B**) Evaluating methionine synthesis activity in response to DMSP. Stationary phase bacteria were supplemented with either 2 μM DMSP or water as control (four biological replicates per condition) and sampled for cell disruption one and two hours after supplementation. Resulting cell crude extracts were used for *in vitro* enzymatic reactions (volume = 1.5 mL; 0.35 mg protein per reaction) with added homocysteine (2 mM) and DMSP (200 μM) to catalyze the formation of 3-*S*-methylmercaptopropionate (3-MMPA), which is the demethylated form of DMSP. Product formation was measured by LC-MS analysis. (**C**) Cell crude extracts of DMSP-supplemented stationary phase bacteria produced slightly more 3-MMPA after 1 hour (p-value = 0.068), and significantly more 3-MMPA after 2 hours (p-value = 0.003), compared to non-supplemented control cultures. Bars represent the mean of four biological replicates (dots), with error bars showing the standard deviation. The Student's t-Test was used to calculate p-values. (**D**) Tracking the metabolic fate of DMSP methyl groups during the lag phase. Freshly initiated bacterial cultures were supplemented with 50 μM [^{13}C-methyl]DMSP, in which both methyl groups are ^{13}C-labeled. The intracellular formation of ^{13}C-labeled metabolites was monitored 2 hours after initiation by LC-MS analysis—a time point at which higher DMSP demethylation activity was observed (shown in **C**). The method identified ^{13}C-labeled SAM (isotope abundance for M+1: 41.6%) and ^{13}C-labeled ^{13}C-labeled *S*-methyl-5'-thioadenosine (MTA; isotope abundance for M+1: 47.9%).

Methyl groups are harvested from DMSP and assimilated into bacterial metabolites during the lag phase through the methionine cycle

To verify the transcriptomics results suggesting the involvement of the methionine cycle in processing harvested methyl groups, we sought direct experimental validation. First, we examined whether bacteria in the stationary phase, before transitioning to the lag phase upon transferring to fresh media, possess the necessary enzymatic machinery to demethylate DMSP, thereby generating methyl groups for use in the methionine cycle. We therefore generated crude cell extracts from stationary phase bacteria supplemented with DMSP (or water as control) for one or two hours. These extracts were then incubated with the substrates required for DMSP demethylation and the utilization of methyl groups in the methionine cycle—homocysteine and DMSP (Fig. 4B). The formation of the demethylated product of DMSP, 3-MMPA, was measured using LC-MS analysis (Fig. 4C). Our results indicate that crude extracts from DMSP-supplemented stationary cells produced more 3-MMPA, with higher levels observed after a longer incubation period with DMSP (2 hours compared to 1 hour). This suggests that exposure to DMSP during the stationary phase influenced the enzymatic demethylation machinery that was subsequently activated in the crude extract (Fig. 4C). Importantly, analysis of the stationary

354 bacteria used to prepare the crude extract showed significantly lower levels of 3-MMPA,
355 regardless of DMSP supplementation (fig. S14). These findings confirm that stationary *P. inhibens*
356 bacteria possess the enzymatic machinery necessary for DMSP demethylation. Furthermore, as
357 bacteria transition from stationary phase to lag phase, this machinery has the potential to become
358 activated and generate available methyl groups.
359
360 To follow the cellular fate of the harvested methyl groups, we wished to identify metabolites that
361 are synthesized from the methyl groups of DMSP during the lag phase. Therefore, bacteria were
362 supplemented with [^{13}C-methyl]DMSP in which both methyl group carbons were labeled. In this
363 experiment, glucose-grown stationary phase bacteria were used to initiate fresh cultures that
364 contained 1 mM glucose as a sole carbon source, and to which either 50 μM [^{13}C-methyl]DMSP
365 or 50 μM unlabeled DMSP were added. Cells were harvested two hours after initiation of fresh
366 cultures (fig. S8)—a time point after which DMSP demethylation activity was higher (Fig. 4C)—
367 and then subjected to metabolite extraction and LC-MS analysis. Our results show that DMSP
368 methyl groups were incorporated into SAM and *S*-methyl-5'-thioadenosine (MTA) with isotope
369 abundances of 41.6% and 47.9%, respectively (values given for M+1 isotopologues with single
370 ^{13}C label; Fig. 4D, fig. S15 and data S4). SAM is formed via the methionine cycle and is required,
371 among others, as a substrate for spermidine synthesis. MTA is a methylated side product of
372 spermidine synthesis (Fig. 4A). The formation of ^{13}C-labeled SAM and MTA supports that DMSP-
373 derived methyl groups are assimilated via the methionine cycle. The percent of isotope abundance
374 was similar for both compounds, suggesting that the majority of MTA is produced from SAM and
375 therefore possesses a similar isotope abundance. We cannot exclude that methyl groups are also
376 used for other processes, such as purine synthesis (fig. S12), however, results of [^{13}C-
377 methyl]DMSP LC-MS analysis are in accordance with the transcriptional upregulation of
378 spermidine synthesis genes in response to DMSP (Fig. 4A). These results demonstrate that DMSP
379 methyl groups are assimilated during the bacterial lag phase through the methionine cycle. These
380 findings corroborate the conclusions drawn from our prior stoichiometric calculations and offer an
381 empirical demonstration of methyl group assimilation through the methionine cycle for the
382 synthesis of essential building blocks.
383
384 *Methylated compounds differentially shorten the lag phase of various bacteria that are*
385 *associated with algae and plants*
386
387 The capacity of *P. inhibens* bacteria to alleviate the cellular demands for methyl groups during the
388 lag phase using algal methylated compounds enables them to initiate earlier growth. This rapid
389 response holds potential significance in environmental settings when various starved bacteria
390 encounter an algal host. Therefore, we hypothesized that the capability to utilize methylated
391 compounds from an external source would be common among algal-associated bacteria. However,
392 for this ability to be advantageous, it should be differentially demonstrated by various bacteria.
393 Our findings indicate that certain algal-associated bacteria exhibit lag phase reduction in response
394 to the methylated compounds DMSP and betaine, though not universally across all species.
395 Additionally, the degree of lag phase reduction differs among bacteria and varies in response to
396 distinct methylated compounds (Table 1, fig. S16).
397
398 The synthesis of methylated compounds is a hallmark of photosynthetic organisms, including both
399 algae and plants[43,44]. Therefore, we tested whether plant-associated bacteria exhibit responses
400 similar to algal-associated bacteria. Our results show that plant-associated bacteria exhibit

401 different lag phase shortening in response to betaine and DMSP (Table 1, fig. S17). We extended
402 our investigation by analyzing the genomes of the tested bacterial strains to determine whether
403 they possess the 83 methyl metabolism genes that exhibited differential expression in *P. inhibens*
404 (Figure 1). However, our analysis did not reveal a correlation between the presence of these genes
405 in the examined genomes and the documented shortening of lag phase (fig. S18). The absence of
406 correlation may be attributed to technical factors such as inadequate annotation and the
407 unavailability of precise genomes for these specific strains. For example, our findings reveal that
408 *Vibrio* bacteria shorten their lag phase in response to DMSP. However, the key DMSP demethylase
409 gene, *dmdA* (gene 25), is absent from the *Vibrio* genome (fig. S18). While previous studies have
410 demonstrated DMSP catabolism in *Vibrio*, the specific enzymes involved remain unidentified[45].
411 These uncertainties emphasize the need for further investigation to elucidate the underlying
412 mechanisms responsible for lag phase shortening across diverse bacterial strains. Our data
413 demonstrate that various bacteria that interact with photosynthesizing organisms can commence
414 earlier growth using methylated compounds of their host. The exact response of bacteria to specific
415 compounds may be influenced by the natural environments in which these bacteria have evolved.
416 These findings illustrate how previously unrecognized bacterial physiologies, such as the
417 mechanism for lag reduction, become apparent when bacteria are studied within an ecological
418 context encompassing factors like starvation and a host.
419
420 **Table 1.** Bacteria that are naturally associated with algae and plants exhibit various lag reduction
421 capabilities in response to DMSP and betaine. Values represent the △lag time of bacteria exposed to 2 μM
422 of DMSP or betaine (compared to controls with water). Values in brackets indicate standard deviation of
423 the difference between estimated means, using three biological replicates per condition. ND: Not detected.
424

Bacterial species	**Lag reduction [hours]**	
	DMSP	**Betaine**
Algal-associated bacteria		
Sulfitobacter pontiacus iR4	1.2 (±0.1)	1.6 (±0.1)
Labrenzia sp. DT40	4.2 (±0.3)	5.6 (±0.3)
Vibrio sp. DT22	1.7 (±0.1)	1.7 (±0.2)
Phaeobacter sp. DT104	2.7 (±0.9)	ND
Pseudoalteromonas sp. DT35	ND	1.4 (±0.1)
Labrenzia sp. DT112	ND	ND
Vibrio sp. DT18	ND	ND
Marinomonas sp. DT74	ND	ND
Plant-associated bacteria		
Bacillus subtilis 168	0.8 (±0.2)	2.1 (±0.1)
Pseudomonas aeruginosa PAO1	1.2 (±0.7)	1.5 (±0.2)

Pseudomonas koreensis PK	1.5 (±0.6)	ND
Ewingella americana EA	ND	ND
Lelliottia amnigena LA	ND	ND
Enterobacter aerogenes Ea	ND	ND

Discussion

The lag phase in the lab and in the environment

More than a century ago, the scientific community identified a non-replicative period when starved bacterial cultures encountered fresh nutrients. This period was termed the "lag phase", and it was observed and characterized in controlled laboratory cultures. However, our understanding of the molecular details of this phase remains limited. The challenge lies primarily in the technical demands of traditional laboratory methodologies, which require high bacterial densities, while the lag phase occurs at the onset of cultures when bacterial populations are exceedingly sparse. Recent advancements have provided insights into the cellular events characterizing the lag phase[15], yet much is unknown about this period in both model and environmental strains.

The complexities of studying the lag phase using laboratory cultures underscore the difficulty in understanding and characterizing this phenomenon in natural microbial populations. Although direct observation of bacterial lag phase in natural settings is impractical, analogies can be drawn between the laboratory-based lag phase and potential occurrences in the environment. In natural settings, bacteria commonly face periods of nutrient scarcity and exist in a phase of nongrowth[46]. Upon encountering a nutrient source, bacteria can resume growth. The transient phase between growth and nongrowth can represent the lag phase. Furthermore, heterotrophic bacteria rely on organic compounds from photosynthetic organisms. These bacteria experience fluctuations in available resources due to diurnal and seasonal photosynthesis variations. The fluctuations lead to cycles of nutrient scarcity followed by surges of organic compounds, potentially triggering a bacterial lag phase during these transitions.

Laboratory model systems cannot fully replicate real-world conditions but can help in assessing the possible environmental relevance of the lag phase. Model system can simulate critical factors such as low bacterial density, nutrient-deprived conditions, low substrate concentrations, and relevant microbial interactions. The utilization of model systems, including simple co-cultures and more complex synthetic communities, can significantly contribute to our understanding of how the lag phase might manifest within natural ecosystems.

Challenges in determining the exact duration of the lag phase

Investigating the lag phase requires the precise definition of its initiation and conclusion. In laboratory settings, the onset of the lag phase is easily determined at the starting of the culture during the inoculation stage. However, pinpointing the termination of the lag phase, specifically when bacteria transition into the growth phase, presents a challenge. Typically, at the population level, the common method for demarcating the lag phase involves plotting bacterial growth

semilogarithmically and identifying the intersection between the initial inoculum level and the extrapolated slope of the logarithmic growth phase. At the single-cell level, the lag phase culminates when a cell reaches its first division. Recent advances in single-cell analysis have unveiled the heterogeneity within microbial populations, with distinct lag phase phenotypes observed within these populations[47].

The common techniques for monitoring bacterial population growth and define their lag phase are further complicated when studying environmental strains. Various environmentally relevant bacteria, such as *P. inhibens*, have mechanisms that enable them to attach onto algal hosts. When multiple bacteria adhere to an algal cell, conventional methods like live counts and optical density measurements may be inadequate for accurately estimating bacterial cell numbers. Therefore, technological advancements to enable the tracking of single bacterial cells while they are attached to their host will be imperative for precision in such studies. In addition, better understanding of the cellular processes that occur during the lag phase may help in developing metabolic and genetic markers for the study of populations and single cells.

Spermidine synthesis and the potential link to translation initiation during the lag phase

Analyses of *P. inhibens* bacteria in the context of their algal host, revealed the centrality of methyl group metabolism during algal-bacterial interactions, and specifically methyl group assimilation during the lag phase. Our data highlights that spermidine synthesis, a downstream metabolite of the methionine cycle, can be a notable cellular sink for methyl groups during the lag phase. In DMSP-supplemented bacteria, pronounced transcriptional upregulation was observed of the *metK* gene that is involved in transforming methionine into SAM[48]—the precursor for spermidine synthesis (Fig. 4A). Additionally, the three most upregulated methyl group metabolism genes were associated with the conversion of SAM into spermidine—a pathway that yields MTA as a side product (genes 1, 2 and 21; fig. S11). Moreover, ^{13}C-labeled methyl groups were incorporated into SAM and MTA during the lag phase (Fig. 4D). Spermidine is a polycationic polyamine that interacts with negatively charged macromolecules and has various cellular functions[42,49]. The benefits of polyamines are often associated with protein synthesis[50], and externally supplemented polyamines can increase protein synthesis by up to 2-fold[49].

Additionally, our results suggest that translation initiation, the crucial step in protein synthesis, could be a destination of methyl groups during lag phase. Translation initiation heavily relies on formylated methionine (fMet) as the initial amino acid. The production of fMet requires at least two C1 groups, emphasizing the importance of methyl groups during the lag phase. In our transcriptome analyses, the *metG* gene that is responsible for charging $tRNA^{Met}$ with methionine, was markedly upregulated in DMSP-supplemented *P. inhibens* bacteria during the lag phase (gene 44; fig. S11). Moreover, we found that various genes involved in adding C1 modifications to tRNA and rRNA components of the translation apparatus were upregulated during the lag phase (e.g., genes 39, 41, 42, 43; fig. S11 and table S3). Thus, while requiring further substantiation, our data suggest a link between methyl group assimilation and translation initiation.

Since protein synthesis is a primary cellular activity during the preparatory lag phase, the functional connection between translation initiation and spermidine synthesis in the context of methyl metabolism warrants additional investigation.

513 *Bacterial lag phase reduction in an environmental context*
514
515 The metabolism of algal-associated bacteria is fueled by algal-produced metabolites. Thus, the
516 bacterial diet naturally includes methylated compounds that are a hallmark for photosynthetic
517 organisms[23–25,43]. Our findings suggest that algal-associated bacteria can efficiently harvest and
518 assimilate methyl groups from algal donor compounds. While bacteria are capable of synthesizing
519 methyl groups from glucose, harvesting methyl groups from host metabolites can provide a cost-
520 effective metabolic shortcut. In the marine environment, expediting the transition from lag phase
521 to exponential growth is critical to compete with other marine bacteria for valuable algal resources.
522 Specifically, we observed that algal produced methylated compounds shortened the lag time by up
523 to 2.5 h in *P. inhibens* (Fig. 2C), which is similar to the doubling time of these bacteria (fig. S7).
524 Consequently, under optimal conditions, bacteria may yield twice as many cells in response to
525 pulses of algal metabolites, compared to bacteria that are not adapted to harvest methyl groups
526 from external methylated compounds. Maximizing the efficiency of resource utilization when
527 resources are available presents a selective advantage to bacteria[51]. Given that different algal hosts
528 synthesize and release a unique composition of metabolites[52,53], including methylated
529 compounds[54,55], the differential bacterial response may represent host-specific adaptations. It
530 remains to be determined how closely the spectrum of methylated compounds generated by
531 specific microalgae corresponds to the demethylation abilities of the associated bacteria.
532 Nevertheless, our study offers an initial demonstration of the tunability of the lag phase,
533 highlighting the existing gap in our understanding of non-growing bacteria and the mechanisms
534 facilitating their transition into growth.

535 **Materials and Methods**

536
537 *Key Resources Table*
538

REAGENT or RESOURCE	SOURCE	IDENTIFIER
Bacterial and algal strains		
Emiliania huxley CCMP3266	Bigelow National Center for Marine Algae and Microbiota (NCMA)	N/A
Phaeobacter inhibens DSM 17395; wild type	German Collection of Microorganism and Cell Cultures (DSMZ)	N/A
Phaeobacter inhibens DSM 17395; *dmdA::aacC1* (Gm^r) KO mutant	This paper	ES146
Vibrio sp. DT22	Despotović *et al.*[56]	N/A
Labrenzia sp. DT40	Despotović *et al.*[56]	N/A
Phaeobacter sp. DT104	Despotović *et al.*[56]	N/A
Pseudoalteromonas sp. DT35	Despotović *et al.*[56]	N/A
Labrenzia sp. DT112	Despotović *et al.*[56]	N/A
Vibrio sp. DT18	Despotović *et al.*[56]	N/A
Marinomonas sp. DT74	Despotović *et al.*[56]	N/A

Sulfitobacter pontiacus iR4	Beiralas *et al*.[57]	N/A
Bacillus subtilis 168	Bacteriology Unit of The Weizmann Institute of Science, Israel	N/A
Pseudomonas koreensis PK	Friedman lab strain collection[58]	N/A
Ewingella americana EA	Friedman lab strain collection[58]	N/A
Pseudomonas aeruginosa PAO1	Friedman lab strain collection	N/A
Lelliottia amnigena LA	Friedman lab strain collection[58]	N/A
Enterobacter aerogenes Ea	Friedman lab strain collection	N/A
Chemicals, peptides, and recombinant proteins		
Yeast extract	Sigma-Aldrich, Merck	Cat#Y1625
Tryptone	Sigma-Aldrich, Merck	Cat#T7293
Sea salts	Sigma-Aldrich, Merck	Cat#S9883
Bacto™ Agar	BD	Cat#214010
L1 Medium Kit - Si (includes f/2 vitamins, L1 trace elements and L1 nutrients solutions)	Bigelow National Center for Marine Algae and Microbiota (NCMA)	Cat#MKL11000L-Si
D-(+)-Glucose	Sigma-Aldrich, Merck	Cat#G7021
Dimethylpropiothetin HCl, ≥ 96.0%, (dimethylsulfoniopropionate, DMSP)	Sigma-Aldrich, Merck	Cat#80828; CAS: 4337-33-1
3-(Methylthio)propionic acid, 98%, (3-*S*-methylmercaptopropionate, 3-MMPA)	Alfa Aesar	Cat#L12861; CAS: 646-01-5
3-Mercaptopropionic acid, 99%, (MPA)	Alfa Aesar	Cat#A13261; CAS: 107-96-0
Sodium propionate, ≥99%	Sigma-Aldrich, Merck	Cat#P1880; CAS: 137-40-6
Sodium acetate, ≥99%	Sigma-Aldrich, Merck	Cat#S5636; CAS: 127-09-3
Choline chloride, ≥98%	Sigma-Aldrich, Merck	Cat#C7527; CAS: 67-48-1
L-Carnitine, ≥98%	Sigma-Aldrich, Merck	Cat#C0158; CAS: 541-15-1
Betaine, ≥99%	Sigma-Aldrich, Merck	Cat#61962; CAS: 107-43-7

N,*N*-Dimethylglycine HCl, 99%	Acros Organics	Cat#204660050; CAS: 2491-06-7
Sarcosine, 98%	Alfa Aesar	Cat#A14594; CAS: 107-97-1
L-Alanine, ≥98%	Sigma-Aldrich, Merck	Cat#A7627; CAS: 56-41-7
Stachydrine HCl, 98%, (proline betaine)	Angene	Cat#AG00ILKM; CAS: 4136-37-2
L-Proline, 99%	Alfa Aesar	Cat#A10199; CAS: 147-85-3
Homarine, ≥95%	Santa Cruz Biotechnology	Cat#sc-470671; CAS: 445-30-7
Trigonelline, 98%	Angene	Cat#AG003V2L; CAS: 6138-41-6
Nicotinic acid, ≥98%	Sigma-Aldrich, Merck	Cat#N4126; CAS: 59-67-6
Gonyol	Kindly provided by Kathleen Thume and Georg Pohnert; synthesized according to Gebser and Pohnert[25]	N/A
Sulfobetaine HCl, (DMSA, dimethylsulfonioacetate, dimethylthetin)	Toronto Research Chemicals	Cat#S699400; CAS: 4727-41-7
L-Cysteine, 98+%	Acros Organics	Cat#173600250; CAS: 52-90-4
Sodium methanthiolate, ≥90% (MeSH)	Sigma-Aldrich, Merck	Cat#71742; CAS: 5188-07-8
Methanol, ≥99.9%	Sigma-Aldrich, Merck	Cat#1060072500; CAS: 67-56-1
Glycine, 99%	Acros Organics	Cat#385900500; CAS: 56-40-6
L-Serine, 99%	Acros Organics	Cat#132660250; CAS: 56-45-1
L-Methionine, 98+%	Acros Organics	Cat#166160250; CAS: 63-68-3
DL-Methionine methylsulfonium Cl, 99%, (*S*-methylmethionine; SMM)	mcule	Cat#MCULE-1226059178; CAS: 3493-12-7
L-Homocysteine, 95%	Angene	Cat#AG0037FN CAS: 6027-13-0
Cell Free Amino Acid Mixture - ^{13}C,^{15}N	Sigma-Aldrich, Merck	Cat#767964
β-Mercaptoethanol, 99%	Sigma-Aldrich, Merck	Cat#M3148 CAS: 60-24-2
n-Hexadecane, 99%	Alfa Aeser	Cat#A10322

Critical commercial assays, kits and consumables		
Buffer RLT	QIAGEN	Cat#79216
Low Binding Silica Grinding Beads (100 µm)	Spex® SamplePrep	Cat#2168
ISOLATE II RNA Mini Kit	Bioline, Meridian Bioscience	Cat#BIO-52072
TURBO™ DNase (2 U/µL)	Invitrogen, Thermo Fisher Scientific	Cat#AM2238
RNAClean XP magnetic beads	Beckman Coulter	Cat#A63987
Qubit™ RNA High Sensitivity (HS) Assay Kit	Invitrogen, Thermo Fisher Scientific	Cat#Q32852
Qubit™ 1X dsDNA High Sensitivity (HS) Assay Kit	Invitrogen, Thermo Fisher Scientific	Cat#Q33230
RNA ScreenTape Analysis	Agilent Technologies	Cat#5067-5576
High Sensitivity D1000 ScreenTape	Agilent Technologies	Cat#5067-5584
riboPOOL depletion kit with Pan-Bacteria probes	siTOOLs Biotech	Cat#dp-K024-000026
riboPOOL depletion kit with *E. huxleyi* probes	siTOOLs Biotech	Cat#dp-K024-000033
FastAP thermosensitive alkaline phosphatase, 1 U/µl	Thermo Fisher Scientific	Cat#EF0651
RNA Clean & Concentrator-5 columns	Zymo Research	Cat#R1015
SuperScript™ IV First-Strand Synthesis System	Invitrogen, Thermo Fisher Scientific	Cat#18091200
T4 RNA ligase 1 (ssRNA Ligase), 30,000 U/ml	New England Biolabs	Cat#M0437M
T4 polynucleotide kinase (PNK), 10 U/µl	New England Biolabs	Cat#M0201S
RNase inhibitor, murine, 40 U/µl	New England Biolabs	Cat#M0314S
SUPERase-IN, 20 U/µl	Invitrogen, Thermo Fisher Scientific	Cat#AM2694
AccuPrime™ *Taq* DNA Polymerase, high fidelity	Invitrogen, Thermo Fisher Scientific	Cat#12346086
NovaSeq 6000 S1 Reagent Kit (100 cycles)	Illumina	Cat#20012865
NextSeq 500/550 Mid Output Kit v2.5 (150 Cycles)	Illumina	Cat#20024904
NucleoSpin Gel and PCR Clean-up Kit	MACHEREY-NAGEL	Cat#740609
Phusion High Fidelity DNA polymerase	Thermo Fisher Scientific	Cat#F530S
QIAprep Spin Miniprep Kit	QIAGEN	Cat#271040
Millex®-GV Filter Unit (Sterile), pore size 0.22 µm	Millipore, Merck	Cat#SLGV033RS
Deposited data		

Co-culture RNA-sequencing reads (dual RNA-seq); demultiplexed, trimmed, QC filtered	This paper	BioProject: PRJNA976961 *Reviewer link:* https://dataview.ncbi.nlm.nih.gov/object/PRJNA976961?reviewer=phsoo22ot32cjn91m99nsqqsvr
Lag phase RNA-sequencing reads; demultiplexed, trimmed, QC filtered	This paper	BioProject: PRJNA977030 *Reviewer link*: https://dataview.ncbi.nlm.nih.gov/object/PRJNA977030?reviewer=sdloe88bnr73kpvmoi1s0ga2e
Emiliania huxleyi CCMP3266 sGenome assembly	Sperfeld *et al.*[59]	https://zenodo.org/record/5702921
Emiliania huxleyi CCMP3266 sGenome annotation version 2	This paper	data S3
Phaeobacter inhibens DSM 17395 genome assembly	Thole *et al.*[60]	assembly accession: GCA_000154765.2
Phaeobacter inhibens DSM 17395 genome annotations (RefSeq)	O'Leary *et al.*[61]	https://ftp.ncbi.nlm.nih.gov/genomes/refseq/bacteria/Phaeobacter_inhibens/latest_assembly_versions/GCF_000154765.2_ASM15476v2/
Phaeobacter inhibens DSM 17395 genome annotations (GenBank)	Thole *et al.*[60]	https://ftp.ncbi.nlm.nih.gov/genomes/genbank/bacteria/Phaeobacter_inhibens/latest_assembly_versions/GCA_000154765.2_ASM15476v2/
Phaeobacter inhibens DSM 17395 KEGG metabolic pathways annotation map	Kanehis and Goto[32]	https://www.genome.jp/pathway/pga01100 (pga01100)

Phaeobacter inhibens DSM 17395 BioCyc annotations (v27.0)	Karp *et al*.[62]	https://biocyc.org/organism-summary?object=GCF_000154765
Oligonucleotides		
1. *dmdA* KO upstream forward primer with homology to pCR™II-TOPO™: GTAACGGCCGCCAGTGTGCTGGAATTCGCCCTTGCCGCCGCATGGCAAACACCG	This paper	N/A
2. *dmdA* KO upstream reverse primer with homology to gentamycin cassette: GCATTACAGTTTACGAACCGAACAGGCTTATGTCAATCAGGTGCTCATGGTTTTGGCGGC	This paper	N/A
3. *dmdA* KO downstream forward primer with homology to gentamycin cassette: GGTGGGCTGCCCTTCCTGGTTGGCTTGGTTTCCGATGCAGTTTGCGTGGTGCG	This paper	N/A
4. *dmdA* KO downstream reverse primer with homology to pCR™II-TOPO™: CCGCCAGTGTGATGGATATCTGCAGAATTCGCCCTTCGCGCGTCGGCGATCTCTG	This paper	N/A
5. *dmdA* KO verification forward primer: GGACGCCATCGCGCTGAAC	This paper	N/A
6. *dmdA* KO verification reverse primer: GGCTGGCTTCTCATGATCTCGC	This paper	N/A
7. Gentamycin cassette forward primer: GTTGACATAAGCCTGTTCG	This paper	N/A
8. Gentamycin cassette reverse primer: GTTAGGTGGCGGTACTTGG	This paper	N/A
9. Gentamycin cassette verification forward primer: GTGCAAGCAGATTACGGTGACG	This paper	N/A
10. Gentamycin cassette verification reverse primer: GAGCCTACATGTGCGAATGATGC	This paper	N/A
Recombinant DNA		
pDN12: *dmdA* KO plasmid (Upstream *dmdA*-Gm-Downstream *dmdA*-TOPOII)	This paper	N/A
pBBR1MCS-5	Kovach *et al*.[63]	N/A
pCR™II-TOPO™	Invitrogen	Cat#K466040
Software and algorithms		
fastq-multx; v1.3.1	Aronesty[64]	https://github.com/brwnj/fastq-multx
Cutadapt; v1.18	Martin[65]	https://anaconda.org/bioconda/cutadapt

STAR; v2.7.5c	Dobin *et al.*[66]	https://github.com/alexdobin/STAR
featureCounts; v2.0.0	Liao *et al.*[67]	https://subread.sourceforge.net/
DeSeq2; v1.36.0	Love *et al.*[68]	https://bioconductor.org/packages/release/bioc/html/DESeq2.html
R; v4.2.0	R Core Team[69]	https://www.R-project.org/
ggplot2; v3.4.1	Wickham[70]	https://ggplot2.tidyverse.org
Growthcurver; v0.3.1	Sprouffske and Wagner[71]	https://github.com/sprouffske/growthcurver
multcomp; v1.4-23	Hothorn *et al.*[72]	https://cran.r-project.org/web/packages/multcomp/index.html
Compound Discoverer™ Software; v3.3	Thermo Fisher Scientific	Cat#OPTON-31061

541 *Microalgae, media composition and general culture conditions*
542
543 The algal strain *Emiliania huxleyi* CCMP3266 was purchased as an axenic culture from the
544 National Center for Marine Algae and Microbiota (Bigelow Laboratory for Ocean Sciences, ME,
545 USA). Absence of bacteria in axenic algal cultures was monitored periodically both by plating on
546 ½ YTSS agar plates (yeast extract, 2 g/L; trypton, 1.25 g/L; sea salts, 20 g/L; agar, 16 g/L) and
547 under the microscope. The absence of bacteria was additionally confirmed by recent transcriptome
548 sequencing[59]. Algae were maintained in ASW_a medium (artificial seawater) at 18°C with a
549 light/dark cycle of 18/6 h and an illumination intensity of 150 mmoles/m^2/s. The ASW_a medium
550 was based on the protocol of Goyet and Poisson[73] and contained mineral salts (NaCl, 409.41 mM;
551 Na_2SO_4, 28.22 mM; KCl, 9.08 mM; KBr, 0.82 mM; NaF, 0.07 mM; Na_2CO_3, 0.20 mM; $NaHCO_3$,
552 2 mM; MgCl · 6 H_2O, 50.66 mM; $CaCl_2$, 10.2 mM, $SrCl_2$ · 6 H_2O, 0.09 mM), f/2 vitamins
553 (thiamine HCl, 100 µg/L; biotin, 0.5 µg/L; vitamin B_{12}, 0.5 µg/L), L1 trace elements (Na_2EDTA ·
554 $2H_2O$, 4.36 mg/L; $FeCl_3$ · $6H_2O$, 3.15 mg/L; $MnCl_2$ · $4H_2O$, 178.1 µg/L; $ZnSO_4$ · $7H_2O$, 23 µg/L;
555 $CoCl_2$ · $6H_2O$, 11.9 µg/L; $CuSO_4$ · $5H_2O$, 2.5 µg/L; Na_2MoO_4 · $2H_2O$, 19.9 µg/L; H_2SeO3, 1.29
556 µg/L; $NiSO_4$ · $6H_2O$, 2.63 µg/L; Na_3VO_4, 1.84 µg/L; K_2CrO_4, 1.94 µg/L) and L1 nutrients ($NaNO_3$,
557 882 µM; NaH_2PO_4 · $2H_2O$, 36.22 µM). The components were dissolved in Milli-Q water (IQ 7003;
558 Merck, Darmstadt, Germany) and the pH adjusted to 8.2 with HCl. Stock solutions of f/2 vitamins,
559 L1 trace elements and L1 nutrients were purchased from the Bigelow Laboratory for Ocean
560 Sciences (Boothbay, ME, USA).
561
562 *Marine bacteria and media composition*
563
564 The bacterial strain *Phaeobacter inhibens* DSM 17395 was purchased from the German Collection
565 of Microorganism and Cell Cultures (DSMZ, Braunschweig, Germany). The bacterial strain
566 *Sulfitobacter pontiacus* iR4 was isolated from a xenic culture of *Emiliania huxleyi* CCMP1516[57].
567 The bacterial strains *Vibrio* sp. DT22, *Labrenzia* sp. DT40, *Phaeobacter* sp. DT104,
568 *Pseudoalteromonas* sp. DT35, *Labrenzia* sp. DT112, *Vibrio* sp. DT18, and *Marinomonas* sp. DT74
569 were isolated from the Mediterranean Sea and Red Sea[56], and belong to the Tawfik lab marine
570 bacteria collection, which is now part of the Segev lab strain collection at the Weizmann Institute
571 of Science, Israel. The marine bacteria were cultivated in ASW_b medium (identical to the ASW_a
572 medium, but with additional 5 mM NH_4Cl and 33 mM Na_2SO_4; f/2 vitamins were omitted, and
573 glucose added as indicated), filtered sea water medium (Mediterranean Sea water enriched with
574 L1 trace elements, f/2 vitamins, and L1 nutrients in the same concentrations as used for ASW_a) or
575 in ½ YTSS medium (yeast extract, 2 g/L; trypton, 1.25 g/L; sea salts; 20 g/L), as indicated.
576 Bacterial isolates were kept at -80ºC in ½ YTSS medium with 20% glycerol for long-term storage.
577
578 *Non-marine bacteria and media composition*
579
580 The bacterial strains *Pseudomonas koreensis* PK, *Pseudomonas aeruginosa* PAO1, *Ewingella*
581 *americana* EA, *Lelliottia amnigena* LA, and *Enterobacter aerogenes* Ea were kindly provided by
582 Jonathan Friedman (The Hebrew University of Jerusalem, Israel)[58]. The *Bacillus subtilis* strain
583 168 was obtained from the Bacteriology Unit of the Weizmann Institute of Science, Israel. The
584 strains were cultivated in M9 medium (Na_2HPO_4 · 7H2O, 64 g/L; KH_2PO_4, 15 g/L; NH_4Cl, 5 g/L;
585 NaCl, 2.5 g/L) with 20 mM glucose. Bacterial isolates were kept at -80ºC in LB medium (tryptone,
586 10 g/L; yeast extract, 5 g/L; NaCl, 10 g/L NaCl) with 20% glycerol for long-term storage.
587

588 *Co-culture RNA-sequencing: Experimental design*
589
590 To analyze the transcriptome of *P. inhibens* DSM 17395 bacteria during co-cultivation with the
591 *E. huxleyi* CCMP3266 algae, a dual RNA-sequencing approach was applied that allows probing
592 prokaryotic and eukaryotic RNA in the same samples, without separating cells by e.g. filtration[74].
593 For cultivation, 250 mL Erlenmeyer flasks with 60 ml ASW_a medium were inoculated with either
594 both organisms (co-cultures), or with one of the two organisms (pure cultures). Specifically, 24
595 flasks were inoculated with both organisms (20,000 *E. huxleyi* cells and 2,000 *P. inhibens* CFUs;
596 bacteria were pre-cultivated for 48 h in ASW_b medium with 2 mM glucose and f/2 vitamins, and
597 added to algae four days after inoculation). Another 24 flasks were inoculated with a pure culture
598 of algae (20,000 *E. huxleyi* cells). All 48 flasks were sealed with aluminum foil and cultivated in
599 standing cultures in a growth room at 18 ºC under a light/dark cycle of 16/8 hr. Illumination
600 intensity during the light period was 150 mmoles/m^2/s. At each sampling point, three random
601 flasks were sacrificed per condition (3 algal-bacterial co-culture flasks, and 3 algal pure culture
602 flasks) and sampled to enumerate algal cells, bacterial colony forming units (CFU) and to harvest
603 cells for RNA extraction (starting from day 0; see fig. S1 for sampling points). Nine additional
604 replicate flasks were inoculated with pure cultures of bacteria (2,000 *P. inhibens* CFUs; 0.88 mM
605 NH_4Cl and 2 mM glucose were added to the ASW_a medium to facilitate bacterial growth). The
606 nine bacterial flasks were cultivated under the same conditions as the flasks with algae. Three
607 flasks were repeatedly sampled to enumerate bacterial CFUs, while three flasks were sacrificed
608 per sampling point to harvest cells for RNA extraction (see fig. S1 for growth curves and RNA
609 sampling points).
610
611 Algal cell numbers were determined for each sampled flask as technical triplicates, using a
612 CellStream flow cytometer (Merck, Darmstadt, Germany). Bacterial CFU numbers were
613 determined for each flask as technical duplicates, using serial plating on ½ YTSS medium agar
614 plates. To harvest cells for RNA extraction, 50 mL culture was centrifuged for 5 min at 18 ºC and
615 3,220 g (5810 R swing-out centrifuge; Eppendorf, Hamburg, Germany) and the supernatant was
616 removed by vacuum suction. Cell pellets were resuspended in 450 µl RLT buffer (QIAGEN,
617 Hilden, Germany) with 1% β-mercaptoethanol, transferred into a 2 mL screw cap tube with 300 mg
618 of 100 µm acid washed Low Binding Silica Beads (SPEX SamplePrep, Metuchen, NJ, USA),
619 plunged into liquid nitrogen and stored at -80 ºC for one month until use.
620
621 *Co-culture RNA-sequencing: RNA extraction and library preparation*
622
623 RNA extracts were generated from 30 selected cell pellets (3 biological replicates per sampling
624 point) that originate from algal-bacterial co-cultures, axenic algae and bacteria grown in pure
625 culture with 2 mM glucose (see fig. S1 for sampling points and sample designations). Cell pellets
626 were disrupted by 5 min bead beating at 30 s^{-1} in a mixer mill MM 400 (Retsch, Haan, Germany).
627 RNA was extracted from disrupted cells using the ISOLATE II RNA Mini Kit, which integrates a
628 step for an on-column DNase treatment (Meridian Bioscience, OH, USA). The extracted RNA was
629 subjected to a second DNAse treatment using the TURBO DNase kit (Thermo Fisher Scientific,
630 Waltham, MA, USA) and subsequently purified with 2x concentrated RNAClean XP magnetic
631 beads (Beckman Coulter, Brea, CA, USA). RNA quantity and integrity was evaluated with the
632 Qubit RNA HS Assay (Invitrogen, Thermo Fisher Scientific, Waltham, MA, USA) and the
633 Tapestation RNA ScreenTape analysis (Agilent Technologies, Santa Clara, CA, USA),
634 respectively (fig. S2). Ribosomal RNA was depleted using the riboPOOL rRNA depletion kit in

combination with Pan-Bacteria probes and custom probes generated for *E. huxleyi* rRNA from the nucleus, plastid and mitochondrion (siTOOLs Biotech, Planegg, Germany). For ribosomal RNA depletion, 0.9 µg of RNA was used as an input with 50 pmol of each of the two depletion probes. After rRNA depletion, RNA was purified with 2x concentrated RNAClean XP magnetic beads (Beckman Coulter, Brea, CA, USA). Subsequent library preparation was performed as described by Avraham *et al*.[74], which is a stranded, poly(A)-independent protocol that targets total RNA. Briefly, depleted RNA was fragmented by heat, treated with DNase and FastAP, and then 3'-tagged by ligating the barcoded adapters 1 to 30[74] (RNase-free HPLC purified; ordered from Integrated DNA Technologies, Coralville, IA, USA). After barcoding, we implemented a calibration sequencing run to quantify the relative abundance of bacterial RNA in each sample. This quantification allows to determine the optimal sample-specific sequencing depths, and prevents over-sequencing of samples that contain either dead algae, or only one of the two organisms. For the calibration RNA-sequencing run, we proceeded with half of the barcoded RNA and stored the rest at -80 ºC. All 30 samples were pooled in an equivolume and purified with RNA Clean & Concentrator-5 columns (Zymo Research, Irvine, CA, USA). RNA was reverse transcribed with the SuperScript IV First-Strand Synthesis System (Invitrogen, Thermo Fisher Scientific, Waltham, MA, USA), using the AR2 primer[74]. The resulting cDNA was 3'-ligated to the 3Tr3 adaptor[74] (HPLC purified; ordered from Integrated DNA Technologies, Coralville, IA, USA). The 3'-ligated cDNA was then amplified with 9 PCR cycles (see fig. S19A for PCR cycle optimization). Finally, the amplified cDNA was purified with a double-sided clean-up step (right: 0.5x, left: 1.5x; RNAClean XP beads, Beckman Coulter, Brea, CA, USA), followed by a left-sided clean-up step (0.7x). The size distribution of the final calibration sequencing library is shown in fig. S19B. After cleanup, the library was sequenced on a NextSeq 500 instrument with a 150 cycles Mid Output Kit (Illumina, San Diego, CA, USA) in paired-end mode (Read 1: 88 bp, Read 2: 78 bp, Index 1: 0 bp, Index 2: 0 bp). Sequencing data were analyzed for the relative abundance of algal and bacterial RNA per sample, using bioinformatics methods described in the section below. The library preparation protocol was then repeated for the final co-culture RNA-sequencing run, starting from the stored, barcoded RNA. The barcoded RNA was pooled in a way that co-culture samples with algae are expected to yield equal amounts of bacterial sequencing reads (fig. S1; co-culture day 04, 06 and 09; expected bacterial feature counts per sample: 250,000-500,000), while fewer sequencing reads were allocated to algal pure cultures (axenic day 04, 06, 09 and 11/12; expected algal feature counts per sample: 40,000,000), co-cultures with bleached algae (co-culture day 11/12; expected algal feature counts per sample: 25,000,000) and bacterial pure cultures (glucose 1 and glucose 2; expected bacterial feature counts per sample: 5,000,000). After reverse transcription and ligation, the 3'-ligated cDNA was amplified with 11 PCR cycles (see fig. S20A for PCR cycle optimization). The final co-culture RNA-sequencing library (fig. S20B) was deep-sequenced on a NovaSeq 6000 instrument with a 100 cycles S2 Kit (Illumina, San Diego, CA, USA) in paired-end mode (Read 1: 64 bp, Read 2: 54 bp, Index 1: 0 bp, Index 2: 0 bp; table S1). The expected distribution of algal and bacterial sequencing reads per sample was confirmed as described below (see table S2 for resulting algal and bacterial feature counts per sample).

Co-culture RNA-sequencing: Data analysis

Illumina raw reads were demultiplexed with fastq-multx[64], allowing one mismatch per barcode (v1.3.1; -m 1). Raw reads were then quality filtered and trimmed with cutadapt[65] (v1.18; -a AGATCGGAAGAGCACACGTCTGAACTCCAGTCAC -A AGATCGGAAGAGCGTCGTGTAGGGAAAGAGTGT -g T{20} -A A{20} --times 2 --nextseq-

682 trim=20 -m 20 --pair-filter=both; see table S2 for summary; reads where deposited under the
683 BioProject accession: PRJNA976961). The quality filtered and trimmed reads were mapped to a
684 reference fasta file that included the previously generated "synthetic genome" assembly
685 (sGenome) of *E. huxleyi* CCMP3266[59] and the genome of *P. inhibens* DSM 17395 (accession:
686 GCF_000154765.2). Read mapping was conducted with STAR[66] (v2.7.5c; --outSAMattributes All
687 --alignIntronMax 5000 --alignMatesGapMax 5000 --outSAMtype BAM SortedByCoordinate --
688 outFilterMultimapNmax 100 --outSAMmultNmax 1). For compatibility with STAR, empty lines
689 generated by cutadapt were replaced with N's (sed 's/^$/N/'). Reads that mapped to *E. huxleyi*
690 features were counted using featureCounts from the subread package[67] (v2.0.0; -p -C -a
691 Ehux3266_sGenome_v2.gff -F GTF -O --fraction; see data S3 for annotation file). Of note, a
692 slightly modified version of the previously generated *E. huxleyi* CCMP3266 annotation file was
693 used with featureCounts[59], in which plastid and mitochondrion annotations were replaced by
694 public annotations (accessions: JN022705.1 and JN022704.1, respectively). For compatibility with
695 featureCounts, the NH:i attribute of STAR bam files was changed to "1" (sed -r 's/NH:i:[0-
696 9]+/NH:i:1/g'; STAR reports the number of alternative alignments in the NH:i attribute, which
697 interferes with featureCounts fractional counting). Reads that mapped to *P. inhibens* features were
698 counted with the same featureCounts options but using the *P. inhibens* RefSeq annotations. The
699 output of featureCounts is summarized in table S2. To evaluate the efficiency of ribosomal RNA
700 depletion, also non-rRNA features were summarized (table S2), in which algal rRNA from the
701 nucleus (*E. huxleyi* CCMP3266 sGenome gene ID: G8853), the plastid (Plas_rrn5, Plast_rrnL,
702 Plast_rrnS) and the mitochondrion (Mito_rrnL, Mito_rrnS), as well as bacterial 23S rRNA
703 (PGA1_RS00070, PGA1_RS12745, PGA1_RS14220, PGA1_RS16070), 16S rRNA
704 (PGA1_RS00055, PGA1_RS12760, PGA1_RS14235, PGA1_RS16085) and 5S rRNA
705 (PGA1_RS00075, PGA1_RS12740, PGA1_RS14215, PGA1_RS16065) were excluded.
706
707 Bacterial gene transcription was analyzed only in co-culture RNA-sequencing samples that
708 contained *P. inhibens* (table S2; fig. S1). Since sample-specific rRNA depletion efficiencies may
709 skew results, bacterial rRNA features were removed from the feature count table for downstream
710 analysis. To analyze sample variability, bacterial non-rRNA feature count results were normalized
711 for sequencing depth and RNA composition using the DESeq2's median of ratios method,
712 followed by a regularized log transformation and principle component analysis[68,75] (v1.36.0; blind
713 = TRUE ; ntop = 500; R version 4.2.0; fig. S3). DESeq2 was further used to identify differentially
714 expressed (DE) genes by comparing samples of bacteria growing with algae (co-culture day 04,
715 06 and 09; figs. S1 and S3) to samples of bacteria growing exponentially in pure cultures
716 (glucose 1; figs. S1 and S3). The apglm method was used to shrink log2 fold changes and account
717 for overweighing of features with low counts and high variability[76]. Shrunken log2 fold changes
718 and adjusted *p*-values are given in the data S1. To compare absolute transcript abundances between
719 genes and samples, bacterial feature counts were converted to transcripts per kilobase million
720 (TPM); a normalization method that accounts for gene length and sequencing depth (data S1). To
721 identify the 20 highest transcribed metabolic genes, the *P. inhibens* feature table (data S1) was
722 filtered for genes that are part of the KEGG metabolic pathways annotation map[32] (pga01100;
723 https://www.genome.jp/pathway/pga01100). The resulting 840 KEGG metabolic genes were
724 filtered for the 20 genes with the highest mean transcript abundances in samples with algae (co-
725 culture day 04, 06 and 09).
726
727 To identify methyl group metabolism genes in *P. inhibens*, publicly available functional
728 annotations were added to the feature table (data S1). These annotations include automatically

729 generated NCBI RefSeq annotations[61], partially curated GenBank submitter annotations[60], KEGG
730 annotations[32], as well as links to BioCyc[62] and the unifying UniProt Archive (UniParc[77]; links
731 redirect to e.g. pre-computed domain annotations at the InterPro database[78]). Features of
732 *P. inhibens* were then filtered for relevant genes, based on differential expression patterns
733 (adjusted *p*-value: ≤ 0.05; log2 fold change: ≤ -0.585 and ≥ 0.585; data S1). The DE-filtered genes
734 were manually curated by sourcing the public annotations, which identified methyl group
735 metabolism genes that are involved in transporting and catabolizing methylated compounds, in
736 harvesting, dissimilating or assimilating one-carbon groups, or in synthesizing tetrahydrofolate
737 (THF). Also genes that are involved in the ethylmalonyl-CoA pathway were included, which
738 replenishes the TCA cycle by capturing CO_2 during growth on the methylated compound DMSP[79].
739 Complementary to this approach, methyl group metabolism genes were identified by revising
740 literature on one-carbon metabolism[80,81], and searching for homologues genes in *P. inhibens* using
741 nucleotide and protein BLAST[82]. In the latter approach, genes were considered as relevant if they
742 exhibited ≥ 50 mean TPM in at least one of the sampling points. The resulting list, which includes
743 83 curated *P. inhibens* methyl group metabolism genes, is given in table S3. For clarification,
744 genes were excluded from the list that did not meet the above-described cut-off filters, such as a
745 putative DMSP cleavage enzyme (*dddP*; PGA1_RS09315) that was poorly transcribed in all
746 samples (< 50 TPM), and non-regulated methyltransferases.
747
748 *Growth response in bacteria to supplements*
749
750 To test the effect of methylated compounds on the growth of *P. inhibens* wild-type and KO mutant
751 with deleted *dmdA* gene (Fig. 3C), bacteria were streaked from glycerol stocks on ½ YTSS medium
752 agar plates and incubated at 30 ºC for 48 hours. After incubation, a single colony was used to
753 inoculate a pre-culture with 10 mL ASW_b medium (1 mM glucose, 100 mL Erlenmeyer flasks).
754 The pre-culture was cultivated at 30 ºC with 130 rpm shaking for 48 hours. After 48 hours, the
755 pre-culture was in the stationary phase and exhibited $OD_{600} \approx 0.1$. The stationary phase pre-culture
756 was used to inoculate the main cultures (1 mL ASW_b medium, 1 mM glucose, start OD_{600} =
757 0.00001 [based on OD_{600} in pre-culture and applied dilution factor]), which contained supplements
758 as indicated (mainly 2 µM of a methylated compound; listed in Key Resources Table).
759 Supplements were prepared as 50 mM stock solutions in Milli-Q water and sterilized by filtration
760 with syringe filters (Millex-GV, 0.22 µm, PVDF, Merck, Darmstadt, Germany). Each inoculated
761 main culture was divided into three or four different wells (biological replicates) of a 96-well
762 microtiter plate (150 µl main culture per well) and overlaid with 50 µl hexadecane to prevent
763 evaporation[83]. Cultivation of the main cultures was conducted at 30 ºC in an Infinite 200 Pro M
764 Plex plate reader (Tecan Group Ltd., Männedorf, Switzerland) with alternating cycles of 4 min
765 shaking and 16 min incubation. Optical density measurements were conducted at 600 nm
766 following the shaking step.
767
768 The same growth protocol was used to analyze growth responses when supplemented with 2 µM
769 of the methylated compounds DMSP or betaine, or water as control in the marine bacteria *Vibrio*
770 sp. DT22, *Labrenzia* sp. DT40, *Phaeobacter* sp. DT104, *Pseudoalteromonas* sp. DT35, *Labrenzia*
771 sp. DT112, *Vibrio* sp. DT18, and *Marinomonas* sp. DT74 (fig. S16). A slightly modified protocol
772 was used for *S. pontiacus* iR4 marine bacteria, in which ASW_b medium was replaced by filtered
773 seawater medium (fig. S16). To study the responses to 2 µM DMSP or betaine, the plant-associated
774 bacteria *B. subtilis* 168, *Pseudomonas koreensis* PK, *Pseudomonas aeruginosa* PAO1, *Ewingella*

americana EA, *Lelliottia amnigena* LA, and *Enterobacter aerogenes* Ea, were grown in M9 minimal media supplemented with 20 mM glucose (fig. S17).

Growth data analysis

For data analysis, microtiter plate absorption values were converted into OD_{600} values by multiplying measured values with a factor of 3,8603. This factor was determined by comparing the absorption (at 600 nm) of a culture sample in a spectrophotometer using a 1 cm cuvette (Ultrospec 2100 Pro, Biochrom, Cambridge, UK) with the absorption in the microtiter plate reader (150 µl culture + 50 µl hexadecane per well). The background absorption, which is the mean absorption during the non-growth phase with stable OD_{600} values (≈ 2-8 hours), was subtracted from each individual well. Results were plotted in R (v4.2.0) using ggplot2 (v3.4.1). For visual aid, smoothing lines were added that average the replicates for each condition (geom_smooth; method: loess). Doubling times and lag times were calculated for each replicate using the Growthcurver package[71] (v0.3.1). For this package, background subtracted OD_{600} values were used as an input that span the time from the lowest to the highest measured absorptions. Growthcurver was used to fit the OD_{600} values into a logistic equation that describes the population size N_t (OD_{600}) at time t. The output of Growthcurver includes the modelled growth rate r, the carrying capacity K, and the initial population size N_0.

$$N_t = \frac{K}{\left[1 + (\frac{K - N_0}{N_0}) \cdot e^{-r \cdot t}\right]}$$

To calculate lag times, we formulated a definition in which lag times equal the time t at which N_t (OD_{600}) reaches an absorption of 0.01. Using this definition, the logistic equation of Growthcurver was rearranged to t and solved with $N_t = 0.01$:

$$t = \left(-\frac{1}{r}\right) \cdot \left[\ln\left(\frac{K - N_t}{K - N_0}\right) - \ln\left(\frac{N_t}{N_0}\right)\right]$$

To calculate △lag times, we first determined the mean lag time for each condition. Then, the mean lag times of supplemented treatment conditions were subtracted from the mean lag time of the control condition. Thus, the resulting △lag times are a measure for the effect of supplements on the length of the lag phase. To determine the standard deviation of the estimated difference between means σ_{M1-M2}, a formula was used that incorporates the standard deviation for the lag time of the treatment condition (σ_1), the control condition (σ_2), and the number of replicates n per condition:

$$\sigma_{M1-M2} = \sqrt{\frac{\sigma_1^2}{n_1} + \frac{\sigma_2^2}{n_2}}$$

Doubling times were calculated by solving the logistic equation of Growthcurver with $N_t = 2N_0$. The R package multcomp[72] (v1.4-23) was used to identify significant differences between lag times and doubling times. Specifically, an ANOVA model (aov function) was fitted to the two growth parameters, followed by a Dunnett's test (glht function).

817
818 *Knock-out mutants with deleted dmdA*
819
820 Primers and plasmids used to generate *P. inhibens* knock-out (KO) mutants are listed in the Key
821 Resources Table. PCR amplification and restriction-free cloning[84] were performed using the
822 Phusion High Fidelity DNA polymerase (Thermo Fisher Scientific, Waltham, MA, USA). PCR
823 products were purified with the NucleoSpin Gel and PCR Clean-up kit (MACHEREY-NAGEL,
824 Düren, Germany). Plasmids were purified with the QIAprep Spin Miniprep Kit (QIAGEN, Hilden,
825 Germany).
826
827 To generate KO mutants for the *dmdA* gene (accession: PGA1_RS19020; gene 25) we first
828 PCR-amplified ~1,000 bp upstream and downstream regions of the respective loci (primers 1-4).
829 A gentamycin resistance gene was amplified from the plasmid pBBR1MCS-5 (primers 7-8). The
830 PCR products (upstream region + gentamycin resistance + downstream region) were then
831 assembled and cloned into the pCR™II-TOPO™ vector (Invitrogen, Thermo Fisher Scientific,
832 Waltham, MA, USA) using restriction-free cloning[84]. This resulted in the KO plasmid pDN12
833 (*dmdA*). For transformation, 10 µg of KO plasmid were added to 300 µl of competent *P. inhibens*
834 cells (prepared by the method of Dower *et al*.[85]), and electroporated with a pulse of 2.5 kV
835 (MicroPulser, Bio-Rad Laboratories, Hercules, CA, USA). Electroporated cells were recovered in
836 2 mL ½ YTSS medium for 12 hours at 30 ºC and transferred to selective ½ YTSS medium agar
837 plates with 30 µg/ml gentamycin. To screen for transformants, single colonies were used as
838 template for PCR reactions (primers 5-6 and 9-10). Gene knock-outs were additionally verified in
839 single-cell clones by Sanger sequencing.
840
841 *Stoichiometric calculations*
842
843 To estimate the amount of methyl group requirements per *P. inhibens* cell during growth on
844 glucose, we identified metabolites that are built from one-carbon (C1) groups[86,87], and are thus C1
845 sinks. The focus was on C1 sinks that are used as building blocks to construct macromolecules
846 such as DNA, RNA and proteins, and for which quantitative data are available in *E. coli*[39]. We
847 identified seven C1 sinks in *P. inhibens* (ATP, GTP, dATP, dGTP, dTTP, histidine and
848 methionine; table S5). Not included were serine, phosphatidylcholine, spermidine, macromolecule
849 methylations and low abundant metabolites. Serine is an important C1 group donor in cells (Fig.
850 1; gene 67), however, serine synthesis from glucose does not consume C1 groups.
851 Phosphatidylcholine has a choline backbone with three *N*-methyl groups and is produced by many
852 bacteria[88]. It was reported that some *Phaeobacter* species produce phosphatidylcholine[89],
853 however, only minor amounts of this lipid were detected in *P. inhibens* DSM 17395 during growth
854 with glucose[90]. The metabolite spermidine was excluded due to uncertainties about methyl group
855 recycling. The bacterium *P. inhibens* possesses all genes required to synthesize spermidine by first
856 decarboxylating *S*-adenosylmethionine (SAM) to *S*-adenosyl 3-(methylsulfanyl)propylamine
857 (dcSAM), and then condensing dcSAM with putrescine to spermidine (Fig. 4A). Importantly, the
858 *S*-methyl group of dcSAM is not directly incorporated into spermidine but remains attached to a
859 side product of spermidine synthesis, which is *S*-methyl-5'-thioadenosine (MTA; Fig. 4A). While
860 the *S*-methyl group of MTA is recycled in other bacteria via the methionine salvage pathway, this
861 pathway appears to be incomplete in *P. inhibens*. Thus, the incomplete methionine salvage
862 pathway may result in the loss of one methyl group per synthesized spermidine molecule.
863 However, considering that a yet unknown methionine salvage pathway may exist in *P. inhibens*[91],

spermidine was not included as a C1 sink (table S5). Methylated forms of the macromolecules DNA[92], RNA[93] and proteins[94] were also not included because to the best of our knowledge, no robust data exist on the quantity of macromolecule methylations in the cell. Lastly, not included were low-abundant C1 sinks such as pantothenate (required for CoA synthesis) or NAD/NADP, which represent negligible fractions of the bacterial biomass[39]. After identifying C1 sinks in *P. inhibens*, we gathered data on the amount of the respective sinks present in *E. coli* (table S5). The values represent *E. coli* cells grown at 37 ºC in aerobic glucose minimal medium and at a doubling time of 40 min[39]. A single *E. coli* cell has a dry weight of 280 fg under these conditions, which we used to calculate the amount of C1 sinks present per cell (amol building block/cell; table S5). We then multiplied the amount of C1 sinks per cell with the net amount of C1 groups that are incorporated into each of the sinks (amol C1 group/cell; table S5). By summing up the results for the individual C1 sinks, we estimated that a single *E. coli* cell requires 190.1 amol C1 groups to synthesize its building blocks. To calculate the C1 group requirement per *P. inhibens* cell, we assumed that *P. inhibens* and *E. coli* produce the same amounts of the respective C1 sinks. This assumption is corroborated by the fact that *P. inhibens* is, like *E. coli*, a copiotrophic bacterium[95] with a single cell length of 1-2 µm[89]. To estimate ATP costs, we retrieved the growth-associated ATP maintenance costs (GAM) from the metabolic model of *P. inhibens*, which is given as 85 mmol ATP per gram dry weight[40]. Based on a dry weight of 280 fg per cell[39], this equals 23,800 amol ATP per *P. inhibens* cell.

Lag phase RNA-sequencing

To analyze transcriptional changes induced by DMSP during the lag phase of *P. inhibens*, a glycerol stock of these bacteria was streaked on a ½ YTSS medium agar plate and incubated at 30 ºC for 48 hours. After incubation, a single colony was used to inoculate four pre-culture flasks, each containing 100 ml ASW_b medium with 1 mM glucose. The four pre-cultures were incubated for 48 hours (30 ºC, 130 rpm shaking), resulting in stationary phase bacteria ($OD_{600} \approx 0.1$). The stationary pre-cultures were then pooled and washed by centrifugation (5 min, 3,220 g and 4 ºC) using a 5810 R swing-out centrifuge (Eppendorf, Hamburg, Germany). After centrifugation, the supernatant was removed by vacuum suction, and pellets were re-suspended in ASW_b medium (without glucose). A second washing step was performed, after which pellets were resuspended in 30 mL ASW_b medium (without glucose) to concentrate the cells. The concentrated cells (OD_{600} = 0.82) were used to inoculate six main culture flasks with DMSP (50 µM) and six flasks without DMSP. Each flask contained 60 mL ASW_b medium (1 mM glucose, pre-warmed at 30 ºC, start OD_{600} = 0.01). The 12 inoculated main culture flasks were incubated at 30 ºC with 130 rpm shaking. Six flasks (three flasks with 50 µM DMSP and three flasks without DMSP) were harvested 15 min after inoculation for RNA extraction. The other six flasks were harvested 40 min after inoculation. Separate cultivation experiments were conducted to confirm that DMSP stimulates growth under the applied conditions (fig. S8). The protocol used for cell harvest and RNA extraction is described in the section *Co-culture RNA-sequencing: RNA extraction and library preparation* with the adaptation that cells were centrifuged at 4 ºC. Results of the RNA extraction are shown in fig. S9. All 12 extracted RNA samples were subjected to RNA library preparation as described in the same section, but with minor modifications. RNA fragmentation was conducted with 300 ng RNA per sample, and rRNA depletion was performed after the pooling step, using 100 pmol Pan-Bacteria probes. Of note, the 3'-ligated cDNA was amplified with 12 PCR cycles (see fig. S21A for PCR cycle optimization). The resulting lag phase RNA-sequencing library (fig. S21B) was sequenced on a NextSeq 500 instrument with a 150 cycles Mid Output Kit

(Illumina, San Diego, CA, USA) in paired-end mode (Read 1: 89 bp, Read 2: 79 bp, Index 1: 0 bp, Index 2: 0 bp; table S6 and S7).

The pipeline described in the section *Co-culture RNA-sequencing: Data analysis* was used to analyze lag phase RNA-sequencing data. Quality filtered and trimmed sequencing reads (deposited under the BioProject accession: PRJNA977030) were mapped to a reference fasta file that contained only the genome of *P. inhibens* DSM 17395 (accession: GCF_000154765.2). After generating the *P. inhibens* non-rRNA feature count table, the data was used as input with the DESeq2 PCA plot function to confirm close clustering of replicates (fig. S10). DESeq2 was also used to compare gene expression in DMSP-supplemented samples with control samples 15 min and 40 min after inoculation (fig. S11). The DE results were included in the TPM normalized non-rRNA feature count table (data S2).

DMSP demethylation from cell crude extracts

Enzymatic DMSP demethylation was measured in cell crude extracts using a method adapted from published protocols[96,97]. A glucose-grown, stationary phase pre-culture of *P. inhibens* bacteria was used to inoculate eight main culture flasks (100 ml ASW_b medium, 5.5 mM glucose). The main cultures were then cultivated for four days (30 ºC, 130 rpm) until reaching stationary phase ($OD_{600} \approx 1.0$). Four stationary phase main culture flasks were supplemented with 2 µM DMSP (100 µl from a sterile 2 mM DMSP stock solution, dissolved in Milli-Q water) while the other four flasks were kept as non-supplemented controls (adding 100 µl Milli-Q water). Cells were harvested 1 hour and 2 hours after supplementation by centrifugation (5 min, 3,220 g, 4 ºC), and pellets were resuspended in 1 mL Solution A (100 mM Hepes-KOH pH 7.5, 1 mM DTT; all steps were conducted on ice, using pre-cooled solutions at 4 ºC). Resuspended cells were then washed twice with Solution A by centrifugation (5 min, 10,000 g, 4 ºC). To disintegrate cell membranes, resuspended cells were transferred into 2 mL screw-capped tubes filled with 600 mg of 100 µm acid-washed Low Binding Silica Beads (SPEX SamplePrep, Metuchen, NJ, USA), plunged into liquid nitrogen, thawed, and disrupted by 5 min bead beating at 30 s^{-1} in a mixer mill MM 400 (Retsch, Haan, Germany). Disrupted cells were centrifuged (5 min, 15,000 g, 4 ºC) and the supernatant transferred into a new tube, resulting in the cell crude extract. Protein concentrations were measured using the Protein Assay Dye Reagent Concentrate (Bio-Rad Laboratories, Hercules, CA, USA), and diluted to 0.7 mg/mL with Solution A. Enzymatic reactions were performed by mixing 0.5 mL of 0.7 mg/mL diluted protein (cell crude extract) with 1 mL of Solution B (20 mM Hepes-KOH pH 7.5, 3 mM homocysteine, 300 µM DMSP, 2 mM DTT), resulting in 0.35 mg protein per 1.5 mL reaction mix. The reaction mixes were incubated for 1 hour at 30 ºC. After incubation, 500 µl of the enzymatic reactions were transferred into fresh tubes, plunged in liquid nitrogen, and lyophilized for subsequent metabolite extraction and LC-MS analysis, as described in the section *Lag phase LC-MS analysis with [13C-methyl]DMSP* (but in negative ionization mode). The identification of 3-MMPA was confirmed by using an authentic standard.

Lag phase LC-MS analysis with [^{13}C-methyl]DMSP

To analyze DMSP methyl group assimilation during the lag phase, [^{13}C-methyl]DMSP, which contained two ^{13}C-labeled methyl groups, was synthesized in the Organic Synthesis Unit, Chemical Research Support, Weizmann Institute of Science, Israel. Labeled [^{13}C-methyl]DMSP

958 was prepared according to Dickschat *et al.*[98]. The synthesis was carried out by the acid-catalyzed
959 addition of [$^{13}C_2$]dimethyl sulfide to acrylic acid, using the experimental conditions described in
960 the literature for the deuterium labelled compound. The ^{13}C-labelling was confirmed by ^{1}H NMR,
961 based on the appearance of the methyl signals as a doublet centered at $\delta = 3$ ppm, the typical ^{1}H-
962 ^{13}C J coupling constant of 145 Hz and the mass spectrum showing the molecular ion at *m/z* 137.
963 The NMR and the mass spectra did not show a signal for unlabeled DMSP.
964
965 Growth conditions for experiments with [^{13}C-methyl]DMSP were comparable to those applied for
966 lag phase RNA-sequencing. Briefly, pre-cultures of *P. inhibens* were cultivated for 48 h (100 ml
967 ASW_b medium, 1 mM glucose) and washed twice by centrifugation. A concentrated pre-culture
968 pool of stationary phase bacteria was used to inoculate eight main culture flasks (60 ml ASW_b
969 medium, 1 mM glucose; start $OD_{600} = 0.01$)—four flasks contained 50 µM [^{13}C-methyl]DMSP
970 and four flasks contained 50 µM non-labeled DMSP. The eight main culture flasks were harvested
971 two hours after inoculation by centrifugation (10 min, 7.000 rpm, 4º C; see fig. S8 for growth
972 curves), and cell pellets were subsequently snap-frozen in liquid nitrogen. The selection of the
973 two-hour time point was informed by the observation of higher DMSP demethylation activity in
974 crude extracts of stationary phase bacteria supplemented with 2 µM DMSP (Fig. 4B).
975
976 Extraction and analysis of polar metabolites were performed as previously described in Malitsky *et*
977 *al.*[99] and Zheng *et al.* with some modifications. The bacterial pellets were extracted with 1 mL of
978 a pre-cooled (-20˚C) homogenous methanol:methyl-tert-butyl-ether (MTBE) 1:3 (v/v) mixture.
979 The tubes were vortexed and sonicated for 30 min in an ice-cold sonication bath (taken for a brief
980 vortex every 10 min). Then, 0.5 mL of a UPLC-grade water:methanol (3:1, v/v) solution with
981 1:500 diluted ^{13}C- and ^{15}N-labeled amino acids standard mix (Sigma-Aldrich, Merck, Darmstadt,
982 Germany) was added to the tubes, followed by vortex and centrifugation. The upper organic phase
983 was discarded. The polar phase was re-extracted with 0.5 mL of MTBE. The lower polar phase
984 was then dried under a gentle stream of nitrogen and kept at -80˚C for metabolite analysis. Dry
985 polar samples were re-suspended in 80 µL Methanol:DDW (50:50) and centrifuged twice to
986 remove the debris. The resuspended samples (40 µL) were transferred to HPLC vials for injection.
987
988 LC-MS metabolic profiling was done as described by Zheng *et al.* with minor modifications.
989 Briefly, analysis was performed using an Acquity I class UPLC System combined with a Q
990 Exactive Plus Orbitrap™ mass spectrometer (Thermo Fisher Scientific, Waltham, USA), operated
991 in a positive and negative ionization modes. The LC separation was done using a SeQuant Zic-
992 pHilic column (150 mm × 2.1 mm) with a SeQuant guard column (20 mm × 2.1 mm; Merck,
993 Darmstadt, Germany). The mobile phase B contained acetonitrile, and the mobile phase A
994 contained 20 mM ammonium carbonate with 0.1% ammonia hydroxide in water:acetonitrile
995 (80:20, v/v). The flow rate was kept at 200 µL/min and the gradient was as follows: 0-2 min 75%
996 of B, 14 min 25% of B, 18 min 25% of B, 19 min 75% of B, for 4 min, 23 min 75% of B. Data
997 processing was done using the Compound Discoverer software (v3.3; Thermo Fisher Scientific,
998 Waltham, USA), when detected compounds were identified by accurate mass, retention time,
999 isotope pattern, and fragments (data S4). The software reports the fractional label incorporation
1000 (exchange rate) after natural abundance correction for each compound. LC-MS data were manually
1001 searched for metabolites involved in methyl group metabolism. This included DMSP, 3-*S*-
1002 methylmercaptopropionate (3-MMPA), *S*-adenosylmethionine (SAM), *S*-adenosyl 3-
1003 (methylsulfanyl)propylamine (dcSAM), *S*-methyl-5'-thioadenosine (MTA), methionine, serine,
1004 glycine, 5-methyltetrahydrofolate, 5,10-methylenetetrahydrofolate, 5,10-

methenyltetrahydrofolate, N^{10}-formyltetrahydrofolate, thymidine-5'-phosphate (dTMP), *S*-methyl-5-thio-D-ribofuranose, *S*-methyl-5-thio-α-D-ribose 1-phosphate (1-PMTR), *S*-Methyl-5-thio-D-ribulose 1-phosphate and ATP. The manual search confirmed the presence of labeled DMSP, SAM and MTA (data S4), which were identified by the MS2 fragmentation patterns.

Bioinformatic analysis of methyl group-related metabolism in algal- associated and plant-associated bacteria

Orthology clusters were employed to assess the presence or absence of methyl group metabolism genes that were identified in *P. inhibenns* (table S3) across the genomes of algal-associated and plant-associated bacteria (Table 1, figures S1 and S17). The analysis was conducted using OrthoFinder[101], which utilizes MCL[102] and FastME[103] algorithms with default settings. Diamond[104] blast results from an all-against-all search served as input data. Reference genomes were utilized in cases where a specific genome was unavailable. The used genomes and their accession numbers are detailed in table S8.

References and Notes

1. Buchan, A., LeCleir, G. R., Gulvik, C. A. & González, J. M. Master recyclers: features and functions of bacteria associated with phytoplankton blooms. *Nat. Rev. Microbiol.* **12**, 686–698 (2014).
2. Cole, J. J., Findlay, S. & Pace, M. L. Bacterial production in fresh and saltwater ecosystems: a cross-system overview. *Mar. Ecol. Prog. Ser.* **43**, 1–10 (1988).
3. Ducklow, H. W., Kirchman, D. L., Quinby, H. L., Carlson, C. A. & Dam, H. G. Stocks and dynamics of bacterioplankton carbon during the spring bloom in the eastern North Atlantic Ocean. *Deep Sea Res. Part II Top. Stud. Oceanogr.* **40**, 245–263 (1993).
4. Field, C. B., Behrenfeld, M. J., Randerson, J. T. & Falkowski, P. Primary production of the biosphere: integrating terrestrial and oceanic components. *Science* **281**, 237–240 (1998).
5. Johnsen, G., Leu, E. & Gradinger, R. Marine micro- and macroalgae in the polar night. in *Polar night marine ecology* (eds. Berge, J., Johnsen, G. & Cohen, J. H.) vol. 4 67–112 (Springer International Publishing, Cham, 2020).

1038 6. Caporaso, J. G., Paszkiewicz, K., Field, D., Knight, R. & Gilbert, J. A. The Western English
1039 Channel contains a persistent microbial seed bank. *ISME J.* **6**, 1089–1093 (2012).
1040 7. Lennon, J. T. & Jones, S. E. Microbial seed banks: the ecological and evolutionary
1041 implications of dormancy. *Nat. Rev. Microbiol.* **9**, 119–130 (2011).
1042 8. Sebastián, M. *et al.* High growth potential of long-term starved deep ocean opportunistic
1043 heterotrophic bacteria. *Front. Microbiol.* **10**, (2019).
1044 9. Needham, D. M. & Fuhrman, J. A. Pronounced daily succession of phytoplankton, archaea
1045 and bacteria following a spring bloom. *Nat. Microbiol.* **1**, 1–7 (2016).
1046 10. Ferrer-González, F. X. *et al.* Resource partitioning of phytoplankton metabolites that support
1047 bacterial heterotrophy. *ISME J.* **15**, 762–773 (2021).
1048 11. Kieft, B. *et al.* Phytoplankton exudates and lysates support distinct microbial consortia with
1049 specialized metabolic and ecophysiological traits. *Proc. Natl. Acad. Sci.* **118**, e2101178118
1050 (2021).
1051 12. Lempp, M., Lubrano, P., Bange, G. & Link, H. Metabolism of non-growing bacteria. *Biol.*
1052 *Chem.* **401**, 1479–1485 (2020).
1053 13. Dworkin, J. & Harwood, C. S. Metabolic reprogramming and longevity in quiescence. *Annu.*
1054 *Rev. Microbiol.* **76**, 91–111 (2022).
1055 14. Jacob, F. & Monod, J. Genetic regulatory mechanisms in the synthesis of proteins. *J. Mol.*
1056 *Biol.* **3**, 318–356 (1961).
1057 15. Bertrand, R. L. Lag phase is a dynamic, organized, adaptive, and evolvable period that
1058 prepares bacteria for cell division. *J. Bacteriol.* **201**, e00697-18 (2019).
1059 16. Rolfe, M. D. *et al.* Lag phase is a distinct growth phase that prepares bacteria for exponential
1060 growth and involves transient metal accumulation. *J. Bacteriol.* **194**, 686–701 (2012).

1061 17. Madar, D. *et al.* Promoter activity dynamics in the lag phase of *Escherichia coli*. *BMC Syst.*
1062 *Biol.* **7**, 136 (2013).
1063 18. Basan, M. *et al.* A universal trade-off between growth and lag in fluctuating environments.
1064 *Nature* **584**, 470–474 (2020).
1065 19. Simon, M. *et al.* Phylogenomics of *Rhodobacteraceae* reveals evolutionary adaptation to
1066 marine and non-marine habitats. *ISME J.* **11**, 1483–1499 (2017).
1067 20. Daly, G. *et al.* Towards a mechanistic understanding of microalgae–bacteria interactions:
1068 integration of metabolomic analysis and computational models. *FEMS Microbiol. Rev.* **46**,
1069 fuac020 (2022).
1070 21. Cooper, M. B. & Smith, A. G. Exploring mutualistic interactions between microalgae and
1071 bacteria in the omics age. *Curr. Opin. Plant Biol.* **26**, 147–153 (2015).
1072 22. Fuhrman, J. A., Cram, J. A. & Needham, D. M. Marine microbial community dynamics and
1073 their ecological interpretation. *Nat. Rev. Microbiol.* **13**, 133–146 (2015).
1074 23. Blunden, G. *et al.* Betaines and tertiary sulphonium compounds from 62 species of marine
1075 algae. *Biochem. Syst. Ecol.* **20**, 373–388 (1992).
1076 24. Keller, M. D., Kiene, R. P., Matrai, P. A. & Bellows, W. K. Production of glycine betaine
1077 and dimethylsulfoniopropionate in marine phytoplankton. I. Batch cultures. *Mar. Biol.* **135**,
1078 237–248 (1999).
1079 25. Gebser, B. & Pohnert, G. Synchronized regulation of different zwitterionic metabolites in the
1080 osmoadaption of phytoplankton. *Mar. Drugs* **11**, 2168–2182 (2013).
1081 26. Bendif, E. M. *et al.* Repeated species radiations in the recent evolution of the key marine
1082 phytoplankton lineage *Gephyrocapsa*. *Nat. Commun.* **10**, 4234 (2019).
1083 27. Segev, E. *et al.* Dynamic metabolic exchange governs a marine algal-bacterial interaction.
1084 *eLife* **5**, e17473 (2016).

1085 28. Abada, A. *et al.* Aerobic bacteria produce nitric oxide via denitrification and promote algal
1086 population collapse. *ISME J.* 1–17 (2023) doi:10.1038/s41396-023-01427-8.
1087 29. Seyedsayamdost, M. R., Case, R. J., Kolter, R. & Clardy, J. The Jekyll-and-Hyde chemistry
1088 of *Phaeobacter gallaeciensis*. *Nat. Chem.* **3**, 331–335 (2011).
1089 30. Bramucci, A. R. & Case, R. J. *Phaeobacter inhibens* induces apoptosis-like programmed cell
1090 death in calcifying *Emiliania huxleyi*. *Sci. Rep.* **9**, 5215 (2019).
1091 31. Thøgersen, M. S., Melchiorsen, J., Ingham, C. & Gram, L. A novel microbial culture chamber
1092 co-cultivation system to study algal-bacteria interactions using *Emiliania huxleyi* and
1093 *Phaeobacter inhibens* as model organisms. *Front. Microbiol.* **9**, (2018).
1094 32. Kanehisa, M. & Goto, S. KEGG: Kyoto Encyclopedia of Genes and Genomes. *Nucleic Acids*
1095 *Res.* **28**, 27–30 (2000).
1096 33. Johnston, A. W., Green, R. T. & Todd, J. D. Enzymatic breakage of
1097 dimethylsulfoniopropionate—a signature molecule for life at sea. *Curr. Opin. Chem. Biol.*
1098 **31**, 58–65 (2016).
1099 34. Moran, M. A., Reisch, C. R., Kiene, R. P. & Whitman, W. B. Genomic Insights into Bacterial
1100 DMSP Transformations. *Annu. Rev. Mar. Sci.* **4**, 523–542 (2012).
1101 35. Gao, C. *et al.* Single-cell bacterial transcription measurements reveal the importance of
1102 dimethylsulfoniopropionate (DMSP) hotspots in ocean sulfur cycling. *Nat. Commun.* **11**,
1103 1942 (2020).
1104 36. Hondorp, E. R. & Matthews, R. G. Methionine. *EcoSal Plus* **2**, (2006).
1105 37. Howard, E. C. *et al.* Bacterial taxa that limit sulfur flux from the ocean. *Science* **314**, 649–
1106 652 (2006).
1107 38. Poolman, B. & Glaasker, E. Regulation of compatible solute accumulation in bacteria. *Mol.*
1108 *Microbiol.* **29**, 397–407 (1998).

1109 39. Neidhardt, F. C., Ingraham, J. L. & Schaechter, M. *Physiology of the Bacterial Cell: A*
1110 *Molecular Approach*. (Springer, Berlin, Heidelberg, 1990).
1111 40. Koblitz, J. *et al.* The metano modeling toolbox MMTB: an intuitive, web-based toolbox
1112 introduced by two use cases. *Metabolites* **11**, 113 (2021).
1113 41. Weiten, A. *et al.* Nanomolar responsiveness of marine *Phaeobacter inhibens* DSM 17395
1114 toward carbohydrates and amino acids. *Microb. Physiol.* **32**, 108–121 (2022).
1115 42. Miller-Fleming, L., Olin-Sandoval, V., Campbell, K. & Ralser, M. Remaining mysteries of
1116 molecular biology: the role of polyamines in the cell. *J. Mol. Biol.* **427**, 3389–3406 (2015).
1117 43. Stefels, J. Physiological aspects of the production and conversion of DMSP in marine algae
1118 and higher plants. *J. Sea Res.* **43**, 183–197 (2000).
1119 44. Rhodes, D. & Hanson, A. D. Quaternary ammonium and tertiary sulfonium compounds in
1120 higher plants. *Annu. Rev. Plant Physiol. Plant Mol. Biol.* **44**, 357–384 (1993).
1121 45. Liu, J. *et al.* Oceanospirillales containing the DMSP lyase DddD are key utilisers of carbon
1122 from DMSP in coastal seawater. *Microbiome* **10**, 110 (2022).
1123 46. Kjelleberg, S., Hermansson, M., Marden, P. & Jones, G. W. The transient phase between
1124 growth and nongrowth of heterotrophic bacteria, with emphasis on the marine environment.
1125 *Annu. Rev. Microbiol.* **41**, 25–49 (1987).
1126 47. Kotte, O., Volkmer, B., Radzikowski, J. L. & Heinemann, M. Phenotypic bistability in
1127 *Escherichia coli*'s central carbon metabolism. *Mol. Syst. Biol.* **10**, 736 (2014).
1128 48. Wei, Y. & Newman, E. B. Studies on the role of the *metK* gene product of *Escherichia coli*
1129 K-12. *Mol. Microbiol.* **43**, 1651–1656 (2002).
1130 49. Igarashi, K. & Kashiwagi, K. Effects of polyamines on protein synthesis and growth of
1131 *Escherichia coli*. *J. Biol. Chem.* **293**, 18702–18709 (2018).

1132 50. Hetrick, B. *et al.* Polyamines accelerate codon recognition by transfer RNAs on the ribosome.
1133 *Biochemistry* **49**, 7179–7189 (2010).
1134 51. Kolter, R., Balaban, N. & Julou, T. Bacteria grow swiftly and live thriftily. *Curr. Biol.* **32**,
1135 R599–R605 (2022).
1136 52. Becker, J. W. *et al.* Closely related phytoplankton species produce similar suites of dissolved
1137 organic matter. *Front. Microbiol.* **5**, (2014).
1138 53. Kujawinski Elizabeth B. *et al.* Metabolite diversity among representatives of divergent
1139 Prochlorococcus ecotypes. *mSystems* **8**, e01261-22 (2023).
1140 54. Heal, K. R. *et al.* Marine Community Metabolomes Carry Fingerprints of Phytoplankton
1141 Community Composition. *mSystems* **6**, e01334-20 (2021).
1142 55. Durham, B. P. *et al.* Chemotaxonomic patterns in intracellular metabolites of marine
1143 microbial plankton. *Front. Mar. Sci.* **9**, 864796 (2022).
1144 56. Despotović, D. *et al.* Utilization of diverse organophosphorus pollutants by marine bacteria.
1145 *Proc. Natl. Acad. Sci.* **119**, e2203604119 (2022).
1146 57. Beiralas, R., Ozer, N. & Segev, E. Abundant Sulfitobacter marine bacteria protect Emiliania
1147 huxleyi algae from pathogenic bacteria. *ISME Commun.* **3**, 1–10 (2023).
1148 58. Kehe, J. *et al.* Positive interactions are common among culturable bacteria. *Sci. Adv.* **7**,
1149 eabi7159 (2021).
1150 59. Sperfeld, M., Yahalomi, D. & Segev, E. Resolving the microalgal gene landscape at the strain
1151 level: a novel hybrid transcriptome of *Emiliania huxleyi* CCMP3266. *Appl. Environ.*
1152 *Microbiol.* **88**, e01418-21 (2022).
1153 60. Thole, S. *et al. Phaeobacter gallaeciensis* genomes from globally opposite locations reveal
1154 high similarity of adaptation to surface life. *ISME J.* **6**, 2229–2244 (2012).

1155 61. O'Leary, N. A. *et al.* Reference sequence (RefSeq) database at NCBI: current status,
1156 taxonomic expansion, and functional annotation. *Nucleic Acids Res.* **44**, D733–D745 (2016).
1157 62. Karp, P. D. *et al.* The BioCyc collection of microbial genomes and metabolic pathways. *Brief.*
1158 *Bioinform.* **20**, 1085–1093 (2019).
1159 63. Kovach, M. E. *et al.* Four new derivatives of the broad-host-range cloning vector
1160 pBBR1MCS, carrying different antibiotic-resistance cassettes. *Gene* **166**, 175–176 (1995).
1161 64. Aronesty, E. Comparison of sequencing utility programs. *Open Bioinforma. J.* **7**, (2013).
1162 65. Martin, M. Cutadapt removes adapter sequences from high-throughput sequencing reads.
1163 *EMBnet.journal* **17**, 10–12 (2011).
1164 66. Dobin, A. *et al.* STAR: ultrafast universal RNA-seq aligner. *Bioinformatics* **29**, 15–21
1165 (2013).
1166 67. Liao, Y., Smyth, G. K. & Shi, W. featureCounts: An efficient general purpose program for
1167 assigning sequence reads to genomic features. *Bioinformatics* **30**, 923–930 (2014).
1168 68. Love, M. I., Huber, W. & Anders, S. Moderated estimation of fold change and dispersion for
1169 RNA-seq data with DESeq2. *Genome Biol.* **15**, 550 (2014).
1170 69. R Core Team. R: A Language and Environment for Statistical Computing. *R Found. Stat.*
1171 *Comput. Vienna Austria URL HttpswwwR-Proj.* (2022).
1172 70. Wickham, H. *Ggplot2: Elegant Graphics for Data Analysis*. (Springer International
1173 Publishing : Imprint: Springer, Cham, 2016). doi:10.1007/978-3-319-24277-4.
1174 71. Sprouffske, K. & Wagner, A. Growthcurver: an R package for obtaining interpretable metrics
1175 from microbial growth curves. *BMC Bioinformatics* **17**, 172 (2016).
1176 72. Hothorn, T., Bretz, F. & Westfall, P. Simultaneous inference in general parametric models.
1177 *Biom. J.* **50**, 346–363 (2008).

1178 73. Goyet, C. & Poisson, A. New determination of carbonic acid dissociation constants in
1179 seawater as a function of temperature and salinity. *Deep Sea Res. Part Oceanogr. Res. Pap.*
1180 **36**, 1635–1654 (1989).
1181 74. Avraham, R. *et al.* A highly multiplexed and sensitive RNA-seq protocol for simultaneous
1182 analysis of host and pathogen transcriptomes. *Nat. Protoc.* **11**, 1477–1491 (2016).
1183 75. Anders, S. & Huber, W. Differential expression analysis for sequence count data. *Genome*
1184 *Biol.* **11**, R106 (2010).
1185 76. Zhu, A., Ibrahim, J. G. & Love, M. I. Heavy-tailed prior distributions for sequence count
1186 data: removing the noise and preserving large differences. *Bioinformatics* **35**, 2084–2092
1187 (2019).
1188 77. The UniProt Consortium. UniProt: the universal protein knowledgebase in 2023. *Nucleic*
1189 *Acids Res.* **51**, D523–D531 (2023).
1190 78. Paysan-Lafosse, T. *et al.* InterPro in 2022. *Nucleic Acids Res.* **51**, D418–D427 (2023).
1191 79. Reisch, C. R. *et al.* Metabolism of dimethylsulphoniopropionate by *Ruegeria pomeroyi* DSS-
1192 3. *Mol. Microbiol.* **89**, 774–791 (2013).
1193 80. Chen, Y. Comparative genomics of methylated amine utilization by marine *Roseobacter*
1194 clade bacteria and development of functional gene markers (*tmm*, *gmaS*). *Environ. Microbiol.*
1195 **14**, 2308–2322 (2012).
1196 81. Chistoserdova, L. Modularity of methylotrophy, revisited. *Environ. Microbiol.* **13**, 2603–
1197 2622 (2011).
1198 82. Altschul, S. F., Gish, W., Miller, W., Myers, E. W. & Lipman, D. J. Basic local alignment
1199 search tool. *J. Mol. Biol.* **215**, 403–410 (1990).
1200 83. Sklodowska, K. & Jakiela, S. Enhancement of bacterial growth with the help of immiscible
1201 oxygenated oils. *RSC Adv.* **7**, 40990–40995 (2017).

1202 84. Peleg, Y. & Unger, T. Application of the Restriction-Free (RF) cloning for multicomponents
1203 assembly. in *DNA Cloning and Assembly Methods* (eds. Valla, S. & Lale, R.) 73–87 (Humana
1204 Press, Totowa, NJ, 2014). doi:10.1007/978-1-62703-764-8_6.
1205 85. Dower, W. J., Miller, J. F. & Ragsdale, C. W. High efficiency transformation of *E. coli* by
1206 high voltage electroporation. *Nucleic Acids Res.* **16**, 6127–6145 (1988).
1207 86. Stauffer, G. V. Regulation of serine, glycine, and one-carbon biosynthesis. *EcoSal Plus* **1**,
1208 (2004).
1209 87. Shetty, S. & Varshney, U. Regulation of translation by one-carbon metabolism in bacteria
1210 and eukaryotic organelles. *J. Biol. Chem.* **296**, 100088 (2021).
1211 88. Geiger, O., López-Lara, I. M. & Sohlenkamp, C. Phosphatidylcholine biosynthesis and
1212 function in bacteria. *Biochim. Biophys. Acta BBA - Mol. Cell Biol. Lipids* **1831**, 503–513
1213 (2013).
1214 89. Martens, T. *et al.* Reclassification of *Roseobacter gallaeciensis* Ruiz-Ponte *et al.* 1998 as
1215 *Phaeobacter gallaeciensis* gen. nov., comb. nov., description of *Phaeobacter inhibens* sp.
1216 nov., reclassification of *Ruegeria algicola* (Lafay *et al.* 1995) Uchino *et al.* 1999 as
1217 *Marinovum algicola* gen. nov., comb. nov., and emended descriptions of the genera
1218 *Roseobacter, Ruegeria* and *Leisingera*. *Int. J. Syst. Evol. Microbiol.* **56**, 1293–1304 (2006).
1219 90. Trautwein, K. *et al.* The marine bacterium *Phaeobacter inhibens* secures external ammonium
1220 by rapid buildup of intracellular nitrogen stocks. *FEMS Microbiol. Ecol.* **94**, fiy154 (2018).
1221 91. Bullock, H. A., Reisch, C. R., Burns, A. S., Moran, M. A. & Whitman, W. B. Regulatory and
1222 functional diversity of methylmercaptopropionate coenzyme A ligases from the
1223 dimethylsulfoniopropionate demethylation pathway in *Ruegeria pomeroyi* DSS-3 and other
1224 proteobacteria. *J. Bacteriol.* **196**, 1275–1285 (2014).

1225 92. Oliveira, P. H. & Fang, G. Conserved DNA methyltransferases: a window into fundamental
1226 mechanisms of epigenetic regulation in bacteria. *Trends Microbiol.* **29**, 28–40 (2021).
1227 93. Höfer, K. & Jäschke, A. Epitranscriptomics: RNA modifications in bacteria and archaea. in
1228 *Regulating with RNA in Bacteria and Archaea* 399–420 (2018).
1229 doi:10.1128/9781683670247.ch23.
1230 94. Murn, J. & Shi, Y. The winding path of protein methylation research: milestones and new
1231 frontiers. *Nat. Rev. Mol. Cell Biol.* **18**, 517–527 (2017).
1232 95. Wünsch, D. *et al.* Amino acid and sugar catabolism in the marine bacterium *Phaeobacter*
1233 *inhibens* DSM 17395 from an energetic viewpoint. *Appl. Environ. Microbiol.* **85**, e02095-19
1234 (2019).
1235 96. Waditee, R. & Incharoensakdi, A. Purification and kinetic properties of betaine-
1236 homocysteine methyltransferase from *Aphanothece halophytica*. *Curr. Microbiol.* **43**, 107–
1237 111 (2001).
1238 97. Smith, L. T., Pocard, J. A., Bernard, T. & Le Rudulier, D. Osmotic control of glycine betaine
1239 biosynthesis and degradation in *Rhizobium meliloti*. *J. Bacteriol.* **170**, 3142–3149 (1988).
1240 98. Dickschat, J. S., Zell, C. & Brock, N. L. Pathways and substrate specificity of DMSP
1241 catabolism in marine bacteria of the Roseobacter clade. *ChemBioChem* **11**, 417–425 (2010).
1242 99. Malitsky, S. *et al.* Viral infection of the marine alga *Emiliania huxleyi* triggers lipidome
1243 remodeling and induces the production of highly saturated triacylglycerol. *New Phytol.* **210**,
1244 88–96 (2016).
1245 100. Zheng, L. *et al.* Fumarate induces redox-dependent senescence by modifying glutathione
1246 metabolism. *Nat. Commun.* **6**, 6001 (2015).
1247 101. Emms, D. M. & Kelly, S. OrthoFinder: phylogenetic orthology inference for comparative
1248 genomics. *Genome Biol.* **20**, 238 (2019).

102. Van Dongen, S. Graph Clustering Via a Discrete Uncoupling Process. *SIAM J. Matrix Anal. Appl.* **30**, 121–141 (2008).

103. Lefort, V., Desper, R. & Gascuel, O. FastME 2.0: A Comprehensive, Accurate, and Fast Distance-Based Phylogeny Inference Program. *Mol. Biol. Evol.* **32**, 2798–2800 (2015).

104. Buchfink, B., Reuter, K. & Drost, H.-G. Sensitive protein alignments at tree-of-life scale using DIAMOND. *Nat. Methods* **18**, 366–368 (2021).

Acknowledgments

General

We appreciate the technical guidance of Dr. Ester Feldmesser, Dr. Bareket Dassa, Dr. Shifra Ben-Dor and Dr. Hadas Keren-Shaul in RNA-sequencing, are thankful for the help of Dr. Ron Rotkopf with statistical analysis, are grateful for the excellent bioinformatic support of Amir Szitenberg, and acknowledge the contribution of Dr. Maxim Itkin with LC-MS analysis (Life Sciences Core Facilities, Weizmann Institute of Science, Israel). We thank Dr. Roi Avraham and Dr. Gili Rosenberg (Weizmann Institute of Science, Israel) for sharing their expertise in dual RNA-sequencing. The compound gonyol was synthesized and kindly provided by Dr. Kathleen Thume and Prof. Georg Pohnert (Friedrich Schiller University, Jena, Germany). We are grateful for inspiring discussions with Dr. Torsten Schubert and Jonathan Hammer (Friedrich Schiller University, Jena, Germany) about cobalamin-dependent one-carbon metabolism, and highly appreciate the stimulating feedback we received from Dr. Elad Noor (Weizmann Institute of Science, Israel), Prof. Uwe Sauer (ETH Zürich, Switzerland), Dr. Anat Bren (Weizmann Institute of Science, Israel) and Dr. Johannes Zimmermann (Christian-Albrechts-University Kiel, Germany) about bacterial metabolism and the lag phase. We are especially thankful for the conceptual guidance and encouragement from the late Prof. Dan Tawfik (Weizmann Institute of Science, Israel) during the early phase of the study.

Funding

M.S. received a Dean of Faculty Fellowship, a Sir Charles Clore Fellowship (Clore Israel Foundation) and a Senior Postdoc Fellowship. D.A.N.B received the Armando and Maria Jinich Fellowship. The study was funded by the Minerva Foundation with funding from the German Federal Ministry for Education and Research, the Israel Science Foundation (ISF 947/18), the European Research Council (ERC StG 101075514) and the de Botton center for marine sciences, granted to E.S.

Author contributions

M.S., D.A.N.B. and E.S. designed the study. M.S., D.A.N.B., S.M., V.F. and L.Y. performed and analyzed experiments. J.R. contributed to the design of the research and helped supervise the project. M.S., D.A.N.B. and E.S. wrote the manuscript. All authors discussed the results and contributed to the final manuscript.

Competing interests

The authors published a patent. Other than that, the authors are not aware of any affiliations, memberships, funding, or financial holdings that might be perceived as affecting the objectivity of this research.

Data and materials availability

All data are available in the main text or the supplementary materials. Further information and requests for resources and reagents should be directed to and will be fulfilled by the lead contact, Einat Segev. Plasmids generated in this study, as well as bacteria that are not deposited in public strain collections, will be made available on reasonable request. RNA-sequencing data have been deposited at the NCBI Sequence Read Archive (SRA) and are publicly available as of the date of publication. Accession numbers are listed in the Key Resources Table. Raw metabolomics data have been deposited to the EMBL-EBI MetaboLights database with the identifier MTBLS9742 and can be accessed here https://www.ebi.ac.uk/metabolights/MTBLS9742.

Supplementary Materials

Figs. S1 to S21

Tables S1 to S8

Data S1 to S4

References for Supplementary Materials